

An-Najah National University
Faculty of Graduate Studies

Studying the Retention of Multivalent Pollutants in Bentonite

By

Isra Sulyman Faiez Maraaba

Supervisor

Dr. Zeid Qamhieh

Co- Supervisor

Dr. Khawla Qamhieh

**This Thesis is Submitted in Partial Fulfillment of the Requirements for
the Degree of Master of Physics, Faculty of Graduate Studies, An-
Najah National University - Nablus, Palestine.**

2014

Studying the Retention of Multivalent Pollutants in Bentonite

By

Isra Sulyman Faiez Maraaba

This thesis was defended successfully on 14/5/2014 and approved by:

Defense Committee Members

Signature

– Dr. Zeid Qamhieh

(Supervisor)



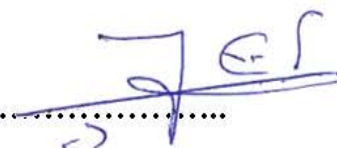
– Dr. Khawla Qamhieh

(Co- Supervisor)



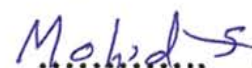
– Prof. Imad Ahmad Barghouthi

(External Examiner)



– Dr. Mohammed Abu- Jafar

(Internal Examiner)



Dedication

بِسْمِ اللَّهِ الرَّحْمَنِ الرَّحِيمِ

{قُنْ إِنَّ صَلَاتِي وَنُسُكِي وَمَحْيَايَ وَمَمَاتِي لِلَّهِ رَبِّ الْعَالَمِينَ}

This Thesis is dedicated to

The soul of my mother (Fatima)

Affectionate father (Sulyman)

Dear husband (Ahmad)

Beloved brothers (Luqman, Hammam and Mohammad)

My nice baby (Omar)

My Muslim Ummah

Acknowledgment

In the name of Allah, the most gracious, the most merciful all praise is to almighty Allah for having guided me all over my life. Acknowledgement is due to An- Najah National university for the great support to this work. My deep appreciation is reserved for thesis supervisors **Dr. Zeid Qamhieh and Dr. Khawla Qamhieh** for their guidance, valuable time and attention they devoted throughout the course of this work. I would like to thank all the physics faculty members who support students in their study and research. My great appreciations are also due to all members of my family and friends who give me the self-confidence to face challenges.

الإقرار

أنا الموقعة أدناه مقدم الرسالة التي تحمل العنوان:

Studying the Retention of Multivalent Pollutants in Bentonite

أقر بأن ما اشتملت عليه هذه الرسالة ، إنما هي نتاج جهدي الخاص ، باستثناء ما تمت الإشارة إليه حيثما ورد ، و أن هذه الرسالة ككل ، و أي جزء منها لم يقدم من قبل لنيل درجة علمية أو بحث علمي لدى أي مؤسسة تعليمية أو بحثية أخرى.

Declaration

The work provided in this thesis, unless otherwise referenced, is the researcher's own work, and has not been submitted elsewhere for any other degree or qualification.

Student's name:

اسم الطالب:

Signature:

التوقيع:

Date:

التاريخ:

VI
Table of Contents

No.	Content	page
	Dedication	III
	Acknowledgment	IV
	Declaration	V
	Table of Contents	VI
	List of Figures	VII
	List of Abbreviations	X
	Abstract	XII
	Chapter One: Introduction	1
1.1	Problem Statement	1
1.2	Sorption Method for Waste Water Purification	2
1.3	Geological Repositories	2
1.4	Clay Minerals	4
1.4.1	Bentonite Clay	5
1.4.2	Sorption Mechanism in Montmorillonite	7
1.5	Literature Review	8
1.6	Research Objectives	12
	Chapter Two: Model and Method	13
2.1	Model	13
2.2	Method	14
2.2.1	Grand Canonical Ensemble	15
2.2.2	Grand Canonical Monte Carlo Simulation	17
2.2.3	The Metropolis method	19
2.2.4	Periodic Boundary Condition	20
2.2.5	Methodology	21
	Chapter Three: Results and Discussion	24
3.1	Bulk Solution Including 100 mM NaCl, 10 mM CaCl ₂ and Radionuclides	24
3.1.1	Fraction of Different Counterions in EDL	25
3.1.2	Effect of Multivalent Cations Concentration in the Bulk Solution	27
3.1.3	Effect of Surface Charge Density	32
3.1.4	Effect of Temperature	34
3.2	Bulk Solution Including 100 mM NaCl, x mM CaCl ₂ and Radionuclides	36
3.3	Bulk Solution Including x mM NaCl, 10 mM CaCl ₂ , and Radionuclides	40
	Chapter Four: Conclusions	46
	References	48
	المخلص	ب

VII
List of Figures

No.	Caption	Page
Figure 1.1	The canister, the bentonite-clay buffer and the crystalline basement	3
Figure 1.2	Structure of Montmorillonite	5
Figure 1.3	Schematic of double layer in a liquid at contact with a negatively charged solid	7
Figure 2.1	Clay model system showing the two clay platelets of negative charge density σ and water slit of thickness h	13
Figure 2.2	Accepting probability as a function of energy change	20
Figure 3.1	Fraction of different counterions in the slit as a function of a) trivalent and b) tetravalent cations concentration in the bulk. The surface charge density has been varied. The slit in equilibrium with a bulk containing 100 mM NaCl, 10 mM CaCl ₂ and and varying amount of multivalent cations. The slit width is 3nm	27
Figure 3.2	Average double layer concentration of a) trivalent and b) tetravalent cations as a function of their bulk concentrations. The surface charge density has been varied. The bulk also contains 100 mM of NaCl and 10 mM of CaCl ₂	28
Figure 3.3	Concentration of counterions as a function of distance from the charged surface. Two different bulk systems are shown with 100 mM Na ⁺ , 10 mM of Ca ²⁺ and a) 0.01 mM of M ⁿ⁺ ions, at surface charge density of -2 e/nm ² b) 0.1 mM of M ⁿ⁺ ions, at surface charge density of -2 e/nm ² . The slit width is 3 nm. Trivalent system(black curves) and tetravalent system (red curves)	29
Figure 3.4	Concentration of tetravalent cations outside the charged surface. The surface charge density is -3 e/nm ² and the bulk solution contains 100 mM of NaCl, 10 mM of CaCl ₂ and varying amount of tetravalent cations as indicated in the graph. The slit width is 3nm	30
Figure 3.5	The retention coefficient of a) trivalent and b) tetravalent cations as a function of the bulk concentrations. The surface charge density has been varied. The bulk also contains 100 mM of NaCl and 10 mM of CaCl ₂	31
Figure 3.6	Average double layer concentration of a) trivalent and b) tetravalent cations as a function of surface charge density of the walls. The bulk contains 100 mM of NaCl and 10 mM of CaCl ₂ and varied concentration of the multivalent cations	32

Figure 3.7	Concentration of counterions as a function of distance from the charged surface. Two different bulk systems are shown with 100 mM Na ⁺ , 10 mM of Ca ²⁺ and 0.01 mM of M ⁿ⁺ ions, at surface charge density of a) -2 e/nm ² b) -3 e/nm ² . Trivalent system (black curves) and tetravalent system (red curves)	33
Figure 3.8	The retention of a) trivalent and b) tetravalent cations as a function of surface charge density of the walls. The bulk contains 100 mM of NaCl and 10 mM of CaCl ₂ and varied concentration of the multivalent cations	34
Figure 3.9	a) Average double layer concentration of multivalent cations as a function of temperature at different values of surface charge densities. The slit in equilibrium with a bulk containing 100 mM NaCl, 10 mM CaCl ₂ and constant amount of multivalent cation. Surface charge density = -4 e/nm ² . b) The retention coefficient of tri- and tetravalent cations as a function of temperature calculated from curves in figure 3.19a. Dots are the simulation results while the solid lines are liner fit	35
Figure 3.10	Fraction of different counterions in the slit as a function of a) trivalent b) tetravalent cations concentration at different bulk solution; 100 mM NaCl + 50 mM CaCl ₂ , 100 mM NaCl + 100 mM CaCl ₂ and 100 mM NaCl + 300 mM CaCl ₂ . The surface charge density has been kept constant at -3 e/nm ² . The slit width is 3nm	37
Figure 3.11	a) Average double layer concentration of multivalent cation as a function of CaCl ₂ concentration at two different surface charge densities. The bulk contains 100 mM NaCl, 1 Mm of multivalent cations and a varying amount of CaCl ₂ .Surface charge density = -4 e/nm ² b) the Retention coefficient calculated from the curves in figure 3.11a. Dots are the simulation results while the solid lines are liner fit or exponential fit	39
Figure 3.12	Average double layer concentration of a) trivalent and b) tetravalent cations as a function of multivalent cations concentration in the bulk. The surface charge density has been kept constant at -3 e/nm ² .The bulk condition has been varied: blue lines = 100 mM NaCl + 50 mM CaCl ₂ , green lines = 100 mM NaCl + 100 mM CaCl ₂ and red lines = 100 mM NaCl + 300 mM CaCl ₂ . The slit width is 3nm	40

Figure 3.13	Fraction of different counterions in the slit as a function of a) trivalent b) tetravalent cations concentration at different bulk solutions; 200 mM NaCl + 10 mM CaCl ₂ , 400 mM NaCl + 10 mM CaCl ₂ and 500 mM NaCl + 10 mM CaCl ₂ . The surface charge density has been kept constant at -3 e/nm ² .The slit width is 3nm	42
Figure 3.14	a) Average double concentration of trivalent cation (black symbols) and tetravalent cation (red symbols) as a function of NaCl concentration. Bulk solution contains 10 mM CaCl ₂ , 0.001 mM of multivalent cations . Surface charge density = -3 e/nm ² . b) The retention coefficient as a function of NaCl concentration calculated from curves in figure 3.14a. Dots are simulation results while solid lines are linear fit	43
Figure 3.15	Average double layer concentration of a) trivalent and b) tetravalent cations as a function of multivalent cations concentration in the bulk. The surface charge density has been kept constant at -3 e/nm ² .The bulk condition has been varied: blue lines = 200 mM NaCl + 10 mM CaCl ₂ , green lines = 400 mM NaCl + 10 mM CaCl ₂ and red lines = 500 mM NaCl + 10 mM CaCl ₂ .The slit width is 3 nm	44
Figure 3.16	Retention coefficient of multivalent cation as a function of a) NaCl concentration, the bulk solution contains 10 mM CaCl ₂ 1mM of trivalent cation and a varying amount of NaCl b) CaCl ₂ concentration, the bulk contains 100 mM NaCl, 1 mM of trivalent cation and a varying amount of CaCl ₂ . The surface charge density is -4 e/nm ² . Dots are simulation results while solid lines are linear fit	45

List of Abbreviations

A	Property as pressure and energy
Al	Aluminum
Am	Americium
As	Arsenic
Bi	Bismuth
c	Ion concentration
C	Column
C[NaCl]	Concentration of NaCl in the bulk solution
C_0	Initial concentration of the solution
Ca^{2+}	Calcium ion
C_B^{n+}	Concentration of a cation with valency n in the bulk solution
$\langle C_{DL}^{n+} \rangle$	Average double layer concentration of a cation with valency
C_e	Equilibrium concentration of the solution
Cm	Curium
Cr	Chromium
D	Metal at the surface
d_{hc}	Hard sphere diameter of the ion
E^-	A surface species
e	Electron charge
E	Solid exchanger
EDL	Electrical Double Layer
Eu	Europium
ϵ_0	Vacuum permittivity
ϵ_r	Relative dielectric permittivity
F	Helmholtz energy
Ga	Gallium
GCMC	Grand Canonical Monte Carlo
h	Planck constant
K^+	Ion in solution
k_B	Boltzmann constant
K_d	Distribution coefficient
Ke	Mass action law coefficient for the reaction
M	Molarity
Mn	Manganese
M^{n+}	Cation with valency n
N	Number of particles
Na^+	Sodium ion
OH	Hydroxyl group
P	Probability
P	Pressure
P-B	Poisson-Boltzmann
Pu	Plutonium
R^+	Ion in solution

XI

S	Entropy
Se	Selenium
Si	Silicon
SKB	Swedish Nuclear Fuel and Waste Management Company
Sn	Tin
T	Temperature
Tc	Technetium
Th	Thorium
V	Volume
W	Probability density
z	Distance from the wall
Ze	Counterion charge
Zr	Zirconium
Λ	Thermal de Broglie wavelength
frac	Fraction
μ	Chemical potential
μ_{ex}	Excess chemical potential
σ	Surface charge density
γ	Retention coefficient
ξ	Random number

XII
Studying the Retention of Multivalent Pollutants in Bentonite
By
Isra Sulyman Faiez Maraaba
Supervisors
Dr. Zeid Qamhieh
Co- Supervisors
Dr. Khawla Qamhieh

Abstract

Radionuclides, even in low concentration, form a potential threat to the environment and, therefore, to humans due to their strong radiation and long half-life times. Water sources are among the targets of contamination by radionuclides. However, for protection of the environment, the removal and recovery of such pollutants represent an important issue of special interest. Adsorption of pollutants on a solid matrix is an effective method used for heavy metal removal from aqueous solutions. In many countries such as Sweden, Canada, France, Spain, Japan etc., the design of radioactive repositories in clay sediments is based on the combination of natural and man-made barriers to gain long-term isolation of nuclear waste. One strong alternative is to put the nuclear waste into copper containers embedded in bentonite and are placed underground.

In this work, the focus is on studying the retention of multivalent pollutants in bentonite clay. The sorption of trivalent and tetravalent radioactive pollutants from sea water on bentonite has been studied using Grand canonical Monto Carlo simulation. Primitive model has been adopted where the water is included by its dielectric constant. Series of simulations have been performed with systematic variations of different parameters to

XIII

investigate the sorption behavior of the system; these parameters including concentration of multivalent ion in the bulk solution, surface charge density of the plates, valency of radioactive ions, temperature of the system and ionic strength.

As a result of this study, the average concentration of multivalent ions in electrical double layer and the retention coefficient are found to be strongly affected by aforementioned parameters. Specifically, the average concentration of multivalent ions in the electrical double layer was found to be increased by increasing the surface charge density, the bulk concentration of radioactive ions and the valency. However, this average concentration was found to be decreased by increasing temperature and ionic strength. On the other hand, the retention coefficient was found to be decreased by increasing the bulk concentration of multivalent species, ionic strength and temperature, although it shows incremental behavior by increasing surface charge density and valency. The predictions of this study about the sorption behavior of multivalent ions well agrees with several experimental results.

Chapter One

Introduction

1.1 Problem Statement

Radionuclides such as Uranium, Thorium, Plutonium, Cesium and others undergo radioactive decays, resulting in the emission of gamma ray(s) and/or particles such as alpha or beta. These emissions represent ionizing radiation that might be harmful to humans by affecting the structure and therefore, the operation of their cells. If the DNA in the nucleus of a cell is damaged, then the cell reproduces in an out-of-control fashion, causing cancer. Also, radiation sickness (Sommers, 2010) is acute radiation syndrome caused by exposure to excessive radiation doses. So, radionuclides form a potential threat to biological environment even in low concentration due to long half-lives and strong radiation.

Substantial amount of radionuclides have been dispersed into atmosphere and biosphere due to human activities in the form of nuclear fission, nuclear power reactors, laboratory experiments and nuclear weapons production. Water sources are among the targets of contamination by radionuclides. The main causes of contamination are accidental leakage and/or planned radioactivity releases through weapon testing or improper handling of radioactive wastes or due to contact of ground water to radionuclides-containing minerals and rocks.

However, due to the importance of pure and clean water to life, the removal of radionuclides from ground water is at present one of the hot topics in many European countries (Lumistea *et al.*, 2012). As an economical and

effective method of waste water purification, sorption of radioactive pollutants by solid adsorbents has been used widely.

1.2 Sorption Method for Waste Water Purification

Sorption is the term used to refer to a variety of processes by which chemical species are fixed on a solid substrate. Sorption process can take several forms that can include fixation of the sorbate at the surface of the sorbent (adsorption) through ion exchange, chemical bonding, or physical attraction forces like van der Waals forces. The term sorption is used also to describe processes in which the sorbate penetrates within the bulk structure of the sorbent (absorption). This term is also occasionally applied to refer to processes in which the sorbate forms a 'coprecipitate' with ions in the sorption medium and deposit on the sorbent interface. Solid adsorbents can be in the form of carbon nanotubes (Li *et al.*, 2002), biosorbent as peat moss (Humelnicu *et al.*, 2010) and dried biomass of *Ascophyllum* (Volesky and Holant, 1995), clay minerals such as bentonite (montmorillonite) (Bartle and Czurda, 1991), metal oxides as Mn-oxides (Debnath *et al.*, 2009), activated carbons (Di Natale *et al.*, 2008) and zeolites as clinoptilolite (Wang *et al.*, 2007).

1.3 Geological Repositories

Building geological repositories deep underground in rocks, salts, or clay sediments in order to store nuclear waste has been used for more than 20 years. The aim of this disposal method is to delay the release of radionuclides to biosphere until their radiological impact is negligible. Clays and their modified forms have received wide consideration for being

used as natural barriers against radioactive migration (Parker and Rae, 1998).

In many countries such as Sweden, Canada, France, Spain, Japan etc., the design of radioactive repositories in clay sediments is based on the combination of natural and man-made barriers to gain long-term isolation of nuclear waste. Swedish nuclear fuel and waste management company (SKB) uses a special method for the final disposal of radioactive pollutants (Jönsson *et al.*, 2009) in which nuclear waste is put into copper canister that is implanted in bentonite clay and placed underground at a depth of about 500 meters as shown in figure 1.1. If the copper canister exposes to corrosion by time, the bentonite clay buffer and the undamaged parts of the canister will hinder water penetration into the canister. In addition, they prevent the leakage of radioactive materials from the canister.

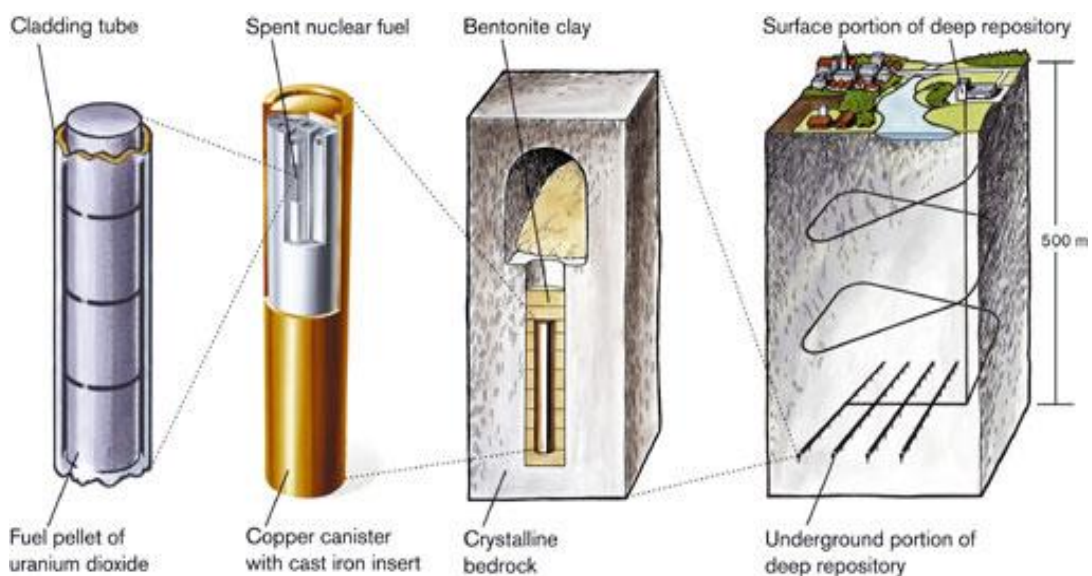


Figure 1.1: The canister, the bentonite-clay buffer and the crystalline basement.

([http://www.skb.se/Templates/ Standard____24109.aspx](http://www.skb.se/Templates/Standard____24109.aspx))

1.4 Clay Minerals

Clay minerals are hydrous aluminum silicates. They have a particle size of less than two micrometers and contain two basic mineral-oxide layers which are piled parallel units of silica and alumina sheets. The first layer is composed of silicon tetrahedral sheets and the second layer is formed of aluminum octahedral sheets. The stacking of these two sheets into layer, the bonding between layers, and the substitution of other ions for Al and Si determine the type of the clay mineral (Meunier, 2005, Rouquerol *et al.*, 1999). There are four groups of clay minerals; kaolinite, illite, vermiculite and smectite. The most common smectite is montmorillonite (Weaver and Pollard, 1973). However, high cation exchange capacity, large specific surface area, layered structure and mechanical and chemical stability make the clays excellent adsorbent materials. Adsorption of radionuclides by clays is affected by several factors such as type of clay, radionuclides, acidity (pH), temperature and ionic strength. Sorption behavior of radionuclides is generally evaluated using the distribution coefficient, K_d (in mL/g), defined as the ratio between the concentration of radioisotope in the clay and the concentration in a solution at equilibrium:

$$K_d = \frac{C_0 - C_e}{C_e} \times \frac{V}{m} \quad (1.1)$$

where C_0 is the initial concentration of the solution (g/L), C_e is the equilibrium concentration of the solution (g/L), V is the volume of the solution (mL) and m is the mass of the clay (g) (Humelnicu *et al.*, 2010).

1.4.1 Bentonite Clay

Dry bentonite is made of nanometric platelets with a thickness approximately one nanometer and lateral dimension of several hundred nanometers. Its basic component is montmorillonite. One platelet of montmorillonite consists of two silica tetrahedral sheets sandwiching a single alumina octahedral sheet and forming the unit cell formula $\text{Al}_2(\text{OH})_2(\text{Si}_2\text{O}_5)_2$ as in figure 1.2. These platelets are stacking together in a way such that oxygen layers of each platelet are adjacent to oxygen of the neighboring platelets forming very weak bonds between the platelets. These weak bonds enable water and polar molecules to intermedate the platelets causing the lattice to expand.

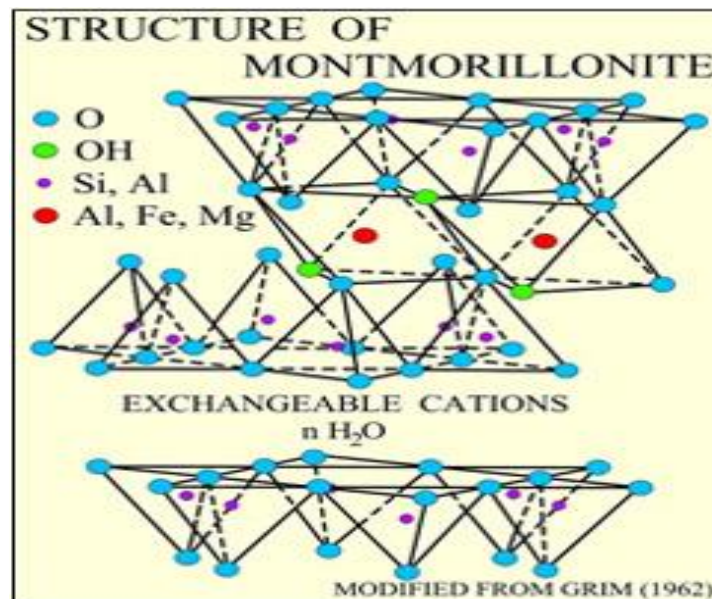


Figure 1.2: Structure of montmorillonite (Grim, 1962).

Bentonite has two surface structures as a result of its layered structure, namely, basal surfaces and edge surfaces. Basal surfaces (i.e. siloxane surface) have permanent negative charge due to isomorphous substitution

of Si^{4+} and Al^{3+} by other lower valence (e.g., Mg^{2+}) cations and its properties is pH independent (Schoonheydt and Johnston, 2006). In contrast, edge surfaces properties are pH dependent. At these surfaces many dangling bonds are found (Lagaly, 2006). In the presence of water the exposed silica or alumina will coordinate with water molecules $\text{D}^+ + \text{H}_2\text{O} \leftrightarrow \text{DOH} + \text{H}^+$ (Stumm, 1992), where D represents a metal at the surface. The resulting surface site, DOH, has a neutral charge. In acidic condition ($\text{pH} < 7$) the surface hydroxyl group may be protonated according to $\text{DOH} + \text{H}^+ \leftrightarrow \text{DOH}_2^+$, so the edge surfaces are positively charged in acid media. On the other hand, in alkaline condition ($\text{pH} > 7$) the edge surfaces are negatively charged as a result of dissociation of the surface hydroxyl groups according to $\text{DOH} \leftrightarrow \text{DO}^- + \text{H}^+$.

The negative charge of bentonite platelets is balanced by interlayer cations such as Na^+ or Ca^{+2} to obtain electroneutrality. These cations can be exchanged with other cations without affecting the clay mineral structure. The platelets form a lamellar structure which usually is modeled as an electrical double layer system.

However, when a charged surface like bentonite is immersed into an electrolyte solution there will be a difference in electrical potential and electrolyte concentration from the aqueous phase to another phase. Charge separation often occurs at the interfacial region due to the different chemical potentials between the two phases. This interfacial region, together with the charged surface, is usually known as the electrical double layer (EDL) (Yang *et al.*, 2004).

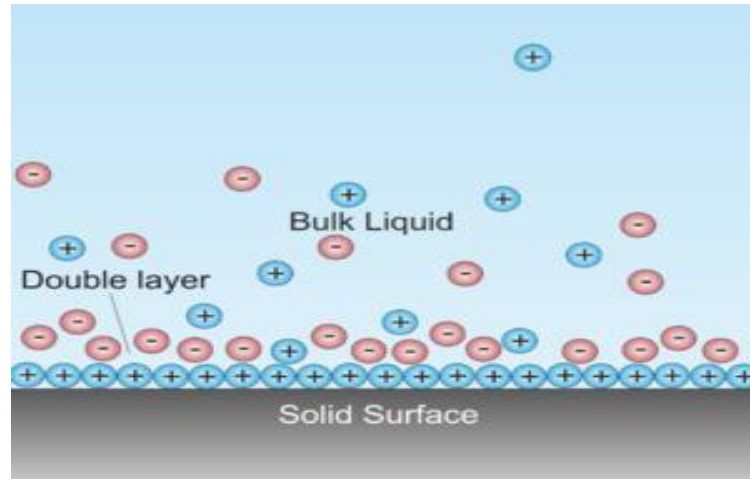
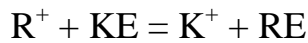


Figure 1.3: Schematic picture of double layer in a liquid at contact with a negatively charged solid.

Bentonite fantastic structure gives it an outstanding properties; large specific surface area, low permeability, high cation exchange capacity and high swelling pressure. These properties enable it to be one of the most promising candidates for using as backfill material in geological repositories.

1.4.2 Sorption Mechanism in Montmorillonite

Montmorillonite can adsorb ions through the processes of ion exchange and surface complexation (Dzombak and Hudson, 1995). Ion exchange process involves an exchange of ions from the surface of the clay with sorbate ions having charges with the same sign but greater affinity. Higher valence ions are preferred, but ions of the same valence have only a minor relative selectivity determined by their hydrated radii. Ion exchange adsorption is pH independent and occurs in the interlayers (basal surfaces) as a result of electrostatic interaction between ions and the negative permanent charge. The ion exchange reaction is always written as



where E is the solid exchanger, R^+ and K^+ represent the ions in solution.

Surface complexation reactions are pH dependent and take place at edge surfaces. They involve construction of chemical bonds between the metal cations, and surface oxygen atoms and OH groups (Jackson, 1998). For example, if E^- is a surface species, therefore, a hypothetical complexation reaction can be written as (Fletcher and Sposito, 1989):



1.5 Literature Review

The sorption capacity of bentonite for the radioactive ions has been studied both experimentally (Humelnicu *et al.*, 2009, Louvel *et al.*, 1993, Turner *et al.*, 1998, Yang *et al.*, 2009) and by simulation (Windt *et al.*, 2004, Bradbury and Baeyens, 2005). Many models have been established to explain the sorption behavior. Ion exchange was described by either a Donnan equilibrium model or diffusive double layers models. In Donnan equilibrium model (Ángeles and Cassou, 2004), the clay particle is represented as a separate homogeneous phase, bearing a negative charge and permeable to small ions rather than macroions. Numerous models were proposed for EDL, such as the Gouy–Chapman model (Hunter, 1985), in which water is considered as a continuum characterized by its relative dielectric permittivity and ions are treated as point charges. Poisson–Boltzmann (P–B) equation (Verwey and Overbeek, 1948) can be used to predict the electrical potential and the concentration distributions. This

model is successful at low surface charge densities and low concentrations of ions. Primitive model (Valleau and Torrie, 1979 & 1982) is prosperous for concentrated electrolyte solutions and higher surface charge densities. In this model, water molecules are also removed and replaced by a dielectric continuum but ions are treated as hard spheres with a point charge implanted at their centers. Monte Carlo simulations have been used to study the primitive model.

A primitive model of EDL was used by Segad et al. (2010) to study the swelling of Na/Ca montmorillonite in the presence of mono and divalent counterions. In that study, large swelling was predicted by Monte Carlo simulations for a clay system in equilibrium with pure water when the clay counterions are monovalent, while in the presence of divalent counterions a limited swelling is obtained. As a consequence of ion-ion correlations a limited swelling of clay takes place in presence of divalent counterions.

The retention of multivalent radioactive species when the polluted aqueous reservoir (ground water) contains several types of cations with different valencies has been studied using Monte Carlo simulations (Qamhieh and Jönsson., The Retention of Multivalent Pollutants in Mineral Layers, in preparation). In that work, in which the primitive model was adopted, the focus was on the importance of electrostatic interactions neglecting any specific chemical interaction. Also, higher surface densities which are more appropriate for cementitious materials were studied. It was chosen to define the ion exchange or competition with a ‘retention coefficient, γ ’ where

$$\gamma = \frac{\langle C_{DL}^{n+} \rangle + C_B^{n+}}{C_B^{n+}} \quad (1.2)$$

$\langle C_{DL}^{n+} \rangle$ is the average double layer concentration of a cation with valency n and C_B^{n+} is concentration of a cation with valency n in the bulk solution. The conclusion of that study is that the retention of multivalent species is increased by increasing the surface charge density or decreasing the ratio Na^+/Ca^{+2} . Otherwise, the retention is decreased by increasing the bulk concentration of multivalent species.

Ion exchange reaction and surface complexation one have been incorporated into such models. Bradbury and Baeyens (1997) established two site protolysis non-electrostatic surface complexation and cation exchange (2 SPNE SC/CE) model. Two different types of surface sites at the interface between the solid and the solution have been considered: (i) $\equiv X^-$ groups carrying a permanent negative charge which explain the cation exchange reaction; (ii) DOH groups that control the surface charge. In that study MINSORB code was used to model the sorption data. This code permitted the uptake of radionuclides by both mechanisms to be calculated at the same time. Kraepiel et al. (1999) developed a thermodynamic model for metal sorption on montmorillonite in which the clay particle, consisting of lamellae and interlayers, is represented as a porous solid bearing a permanent negative charge with an infinite plane interface (i.e. edges) with the solution. Because of the negative potential of the clay, cation exchange occurs inside the clay particle. Surface complexation reactions occur at the interface. In that study calculations have been done on the potential in the bulk of the clay and near the interface, as well as the surface potential–surface charge density relation.

The sorption properties of tri- and tetravalent radioactive ions on bentonite have been the subject of many studies performed in order to understand the effects of the factors affecting the sorption process. These factors include time, temperature, pH, ionic strength, concentration of radioactive elements.... etc.

Multiple batch experiments were performed to study the effect of pH of the solution on the retention of multivalent ions in bentonite. The sorption of Cr(III) (Khan *et al.*, 1995), As(III) (Manning and Goldberg, 1996) Am(III) (Yu *et al.*, 2012), Bi(III) (Ulrich and Degueldre, 1993), Cm(III) (Grambow *et al.*, 2006) and Eu(III) (Songsheng *et al.*, 2012) increases by increasing pH of the solution. While the sorption of Ga(III) (Benedicto *et al.*, 2013) shows a decreasing tendency. On the other hand, the distribution coefficients of some tetravalent ions such as Zr(IV) (Allard *et al.*, 1979), Se(IV) (Shi *et al.*, 2013), Tc(IV) (Baston *et al.*, 1995) and Sn(IV) (Oda *et al.*, 1999) decrease by increasing pH of the solution. The sorption of Th(IV) (Zhao *et al.*, 2008) on bentonite increases for pH =1 to 4 and remains constant otherwise. By increasing pH of the solution, Pu(IV) (Lujanienė *et al.*, 2007) sorption on bentonite increases and reaches maximum value beyond which it decreases again.

Temperature is one of the factors that affect the sorption of multivalent ions on bentonite. The retention of Am(III) (Yu *et al.*, 2012) and Cm(III) (Grambow *et al.*, 2006) on bentonite increases by increasing temperature. On the other hand, the sorption of Cr(III) (Khan *et al.*, 1995) inhibits by

increasing temperature. The distribution coefficient of Th(IV) (Zhao *et al.*, 2008) has a decreasing behavior with increasing temperature.

Various experiments were also carried out in order to investigate the sorption behavior of radioactive ions on bentonite as a function of ionic strength. Am(III) (Yu T., 2012) and Cr(III) (Khan *et al.*, 1995) sorption on bentonite decreases by increasing ionic strength, while Eu(III) (Songsheng *et al.*, 2012) and Bi(III) (Ulrich and Degueldre, 1993) retention are ionic strength independent. Th(IV) (Zhao *et al.*, 2008) sorption data indicates that the sorption of Th(IV) is decreasing by increasing the ionic strength.

Increasing the concentration of multivalent cation on solution affects its sorption on bentonite. The sorption of Cr(III) (Khan *et al.*, 1995) and Sn(IV) (Monika *et al.*, 2007) on bentonite is decreasing as a function of their concentration.

1.6 Research Objectives

The objectives of this work can be summarized in the following points:

1. Studying the retention (sorption) of tri- and tetravalent ions when the polluted aqueous reservoir contains several types of cations with different valencies.
2. Investigating the effect of salt concentration, the surface charge density, and the temperature on the retention of multivalent radioactive species in bentonite by using Monte Carlo simulations.
3. Comparing the obtained simulation results to the available experimental ones.

Chapter Two

Model and Method

2.1 Model

Montmorillonite has a lamellar structure that can be described by a simple model system shown in figure 2.1. In this model, two clay platelets would be treated as two infinite plane surfaces with a uniform negative charge density, σ , separated by a narrow water slit of thickness h and containing neutralizing counterions and added salts. The lamellae are in contact with an infinite salt reservoir of known salt concentration (bulk solution) at an equilibrium condition.

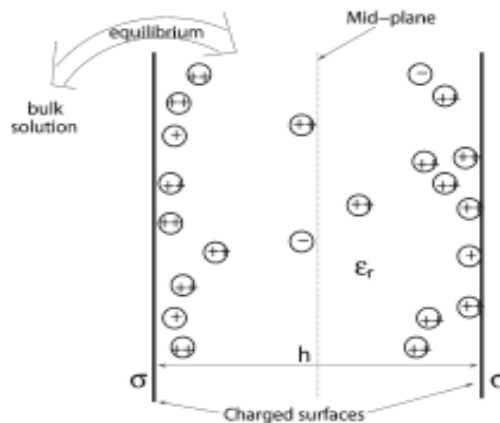


Figure 2.1: Clay model system showing the two clay platelets of negative charge density σ and water slit of thickness h .

The familiar primitive model (Valleau and Torrie, 1979 & 1982) is used to model electrolyte solution where water is considered as dielectric continuum with a relative dielectric permittivity, $\epsilon_r = 78$. The ions are represented by hard spheres with a point charge implanted at their centers.

The potential energy $U(r_{ij})$ between ions i and j separated by a distance r_{ij} , is given by:

$$U(r_{ij}) = \frac{q_i q_j e^2}{4\pi\epsilon_r \epsilon_0 r_{ij}} \quad r_{ij} > d_{hc} \quad (2.1)$$

$$U(r_{ij}) = \infty \quad r_{ij} \leq d_{hc} \quad (2.2)$$

Where q_i is the ion valency, e is the elementary charge (1.6×10^{-19} C), ϵ_0 is the vacuum permittivity (8.85×10^{-12} C²/N.m²) and d_{hc} is the hard sphere diameter of the ion. Due to interaction of ions with the charged wall, potential energy of interaction is developed between the ions at distance z from the wall and is given by:

$$U(z) = -2\pi \sigma q_i e |z| / \epsilon_r \epsilon_0 \quad (2.3)$$

From symmetry, it can be concluded that the sum of the ion-wall potentials is independent of the ion's position between the walls. Consequently, these energies are not required in generating the Markov chain (Brémaud, 1999). The interaction ranging outside the simulation box is taken into account by including the external potential (Jönsson *et al.*, 1980). In this model, image charges are not included which means that there is no dielectric discontinuity at the surfaces. In addition, periodic boundary conditions (Metropolis *et al.*, 1953) were applied in the directions parallel to the surfaces.

2.2 Method

Computer simulations have been developed to be an additional way of doing scientific research. In some cases simulations supply a theoretical

basis for understanding experimental results, and in other instances simulations provide ‘experimental’ data with which theory may be compared. Therefore, the properties of many particle systems have been studied using molecular simulation. The restriction of simulation is how precisely the mathematical model can express the behavior of the system of interest and the information being collected from the simulation. However, data obtained by simulation can be less expensively, less dangerously and the cost is limited to the computer time and its memory.

Monte Carlo simulation (Metropolis *et al.*, 1953), is an example of molecular simulations methods, which pursues random generation of configurations and relies on the positions of the particles. Metropolis *et al.* (1953) carried out the first simulation of liquids using the Monte Carlo method. Monte Carlo simulations are computerized model sampling experiments which comprise the generation of random numbers followed by arithmetic and logical operations. Moreover, Monte Carlo method is used to simulate various thermodynamics ensembles such as the canonical ensemble, the isothermal-isobaric ensemble, and the grand canonical ensemble.

2.2.1 Grand Canonical Ensemble

Ensemble is a virtual collection of a very large number of systems, each of which represents a possible state in which the real system might be (McQuarrie, 2003). In grand canonical ensemble each system is enclosed in a container whose walls are heat conducting and permeable to the passage of molecules. In this ensemble the temperature (T), volume (V) and

chemical potential (μ) are fixed but the number of molecules is varied so it is called constant- μ VT ensemble.

The chemical potential is the derivative of the Helmholtz free energy (F) with respect to particle number (N) when temperature and volume are held constant:

$$\mu = \left(\frac{dF}{dN} \right)_{T,V} \quad (2.4)$$

where the Helmholtz free energy is defined as:

$$F = U - TS \quad (2.5)$$

in which U is the internal energy of the system, and S is the entropy. Mainly, μ is the amount by which the free energy will change if we add another particle to the system while holding the volume and temperature constant. However, for two phases coexistence, the chemical potential must be the same for both phases. The particles diffuse from one phase to another until the chemical potentials are equalized. Thus, equal chemical potentials are a stability condition for phase coexistence.

Grand canonical ensemble is used in adsorption studies (Whitehouse *et al.*, 1983). In the experimental system, the adsorbed ions are in equilibrium with the ions in the reservoir i.e. the temperature and chemical potential of the ions inside and outside the adsorbent are equal. In simulation, the bulk solution that is in contact with the lamellae (adsorbent) can be considered as a reservoir that forces a temperature and chemical potential on the adsorbed ions. So, it is enough to know the temperature and chemical

potential of the reservoir to determine the equilibrium concentration of ions inside the adsorbent.

The grand canonical partition function is given by (Allen and Tildesley, 1987):

$$Q_{\mu VT} = \sum_N \frac{1}{N! h^{3N}} \exp(\beta \mu N) \int dr dp \exp(-\beta H) \quad (2.6)$$

Where $\beta = (1/k_B T)$, k_B is Boltzmann constant, N is the number of particles, H is the Hamiltonian, p is the momentum, r is the radial distance and h is Planck's constant.

The average of a property A is given by (Allen and Tildesley, 1987):

$$\langle \mathbf{A} \rangle_{\mu VT} = \frac{\sum_{N=0}^{N=\infty} (\Lambda^{3N} N!)^{-1} V^N \exp(\beta \mu N) \int ds A(s) \exp(-\beta U(s))}{Q_{\mu VT}} \quad (2.7)$$

where Λ is the thermal de Broglie wavelength which is given by:

$$\Lambda = (h^2/2\pi m k_B T)^{1/2} \quad (2.8)$$

With (s) is a set of scaled coordinates (s_1, s_2, \dots, s_n) defined for each particular value of N as

$$s = \frac{r}{L} \quad (2.9)$$

where L is the size of the simulation box.

2.2.2 Grand Canonical Monte Carlo Simulation

In a grand canonical Monte Carlo (GCMC) simulations (Frenkel and Smit, 1996), it is necessary to generate a sequence of random states so that by the end of the simulation each state has occurred with the appropriate

probability. This is done by set up a Markov chain which is a series of trials with outcomes belonging to the same state space. Whereas, the outcome of each trial relies only on the outcome of the trial that directly precedes it. In GCMC simulations, the Markov chain is constructed so that the limiting distribution is proportional to the probability density (W) given by (Frenkel and Smit, 1996):

$$W = \exp(-\beta(U(s) - N\mu) - \ln N! - 3N \ln \Lambda + N \ln V) \quad (2.10)$$

A number of methods of generating this chain have been proposed. Most workers now adopt the original method of Norman and Filinov (Norman and Filinov, 1969). In this technique there are three different types of move:

(1) Displacement of particles: A particle is selected randomly and is given a new random displacement. Assuming the interaction potential before the move is U_m and the potential after is U_n , therefore,

$$\Delta U_{nm} = U_n - U_m$$

This move is accepted with a probability, P ,

$$P = \min [1, \exp \{-\beta (\Delta U_{nm})\}] \quad (2.11)$$

$P = 1$ if ΔU_{nm} is negative, and $P < 1$ if ΔU_{nm} is positive.

(2) Trial creation: The ions are inserted randomly and the creation of a particle is accepted with a probability

$$P = \min [1, \frac{V}{\Lambda^3(N+1)} \exp \{\beta (\mu - \Delta U_{nm})\}] \quad (2.12)$$

(3) Trial destruction: A particle is removed randomly and the removal of a particle is accepted with a probability

$$P = \min \left[1, \frac{N\Lambda^3}{V} \exp \{-\beta (\mu + \Delta U_{nm})\} \right] \quad (2.13)$$

In any type of moves, if $P = 1$, the new configuration is accepted and added to the ensemble. If $P < 1$, then it is decided by the Metropolis method (Metropolis *et al.*, 1953) discussed in the following section.

Thus the displacement, the destructions, and the creations are selected randomly, with equal probability (i.e. we move a particle 1/3 of the time, create a particle 1/3 of the time, and destroy a particle 1/3 of the time). Adding to or deleting ions from the system will be as a neutral pair.

2.2.3 The Metropolis method

If the above calculated probability P is less than 1, a random number ξ is generated uniformly on $[0, 1]$. If $\xi < P$, then the move is accepted and added to the ensemble; if $\xi > P$, then the move is rejected (Metropolis *et al.*, 1953). For example, If a particle is given a random displacement and as a consequence there is an increase in the potential energy of configuration ΔU_0 , then a random number is generated. If the generated random number is ξ_1 as shown in figure 2.2, then the trial is accepted. But, if the random number is ξ_2 , then the trial is rejected.

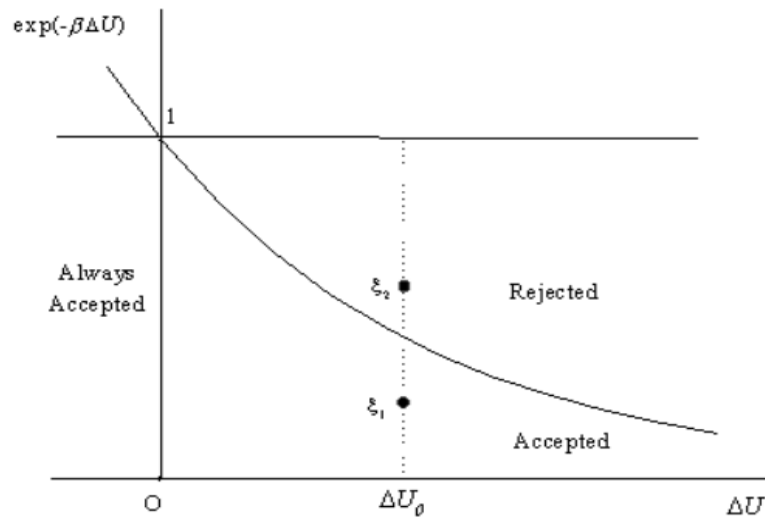


Figure 2.2: Accepting probability as a function of energy change.

2.2.4 Periodic Boundary Condition

In order to overcome the problem of surface effects, the complete substance is supposed to be periodic (Metropolis *et al.*, 1953), consisting of many parallelepiped boxes forming an infinite lattice; each box containing N ions in the same configuration with a dimension $L \times L \times W$. During simulations, as a molecule moves in the central box, its periodic image in each of the boxes moves in exactly the same way. Thus, if a molecule leaves the central box, one of its images will enter the box through the opposite face. The number of molecules in the central simulation box is conserved during a trial displacement.

As a consequence of periodic boundary condition, the energy calculations of a particular configuration were done in the minimum image approximation (Allen and Tildesley, 1987) in which the potential energy of a particle is evaluated by summing the pair interactions with only one

image of each of the other particles, that is the image closest to the particle in question.

In computer simulation, the radial distribution function $g(r)$ is usually calculated assuming periodic boundary condition. Where $g(r)$ is the probability that two particles are a distance r apart:

$$g(r) = \left(1 - \frac{1}{N}\right) \left\langle \sum_{i < j} \delta(r - |r_i - r_j|) \right\rangle$$

2.2.5 Methodology

In this study, Monte Carlo simulation was applied in order to go beyond the mean field approximation inherent in the Poisson-Boltzmann equation. However, this kind of simulation was carried out with Metropolis algorithm in grand canonical ensemble (μVT), where the lamellar system is in equilibrium with salt reservoir of finite concentration (bulk electrolyte). In this case, the concentration of a species in the double layer and in a bulk can differ, but the chemical potentials are equal. In order to investigate the retention of highly charged species, a bulk has been constructed with a reasonable concentration of a normal species, NaCl and CaCl₂, plus a small amount of a trivalent (M^{3+}) or tetravalent (M^{4+}) ion in low concentration. However, in the presence of several types of counterions, i.e. different valencies, there will be a competition of charged surface. The different counterions will contribute to the neutralization of the charged surface, but to strongly varying degree.

The chemical potential needed for the GCMC simulations' input were determined by the iterative-GCMC algorithm (Malasics *et al.*, 2008) in which the chemical potential (μ) can be written as a sum of standard part, an ideal part and an excess part as follows:

$$\mu = k_B T \ln \Lambda^3 + k_B T \ln c + \mu_{ex} \quad (2.14)$$

Where c is the ion concentration and μ_{ex} the excess chemical potential. In grand canonical ensemble, the total chemical potential for the bulk and for the electrical double layer is equal. As a result of electrostatic interaction, μ_{ex} for bulk and μ_{ex} for double layer can be quite different (Guldbrand *et al.*, 1984).

The Monte Carlo box was a parallelepiped with a dimensions $L \times L \times W$ with one dimension (W) determined by the separation h between the charged surfaces, while the extension of the box in the lateral directions follows from the surface charge density σ , the counterion charge Ze , and the number of counterions N . A series of simulations were performed at a constant distance between the plates of 3nm.

Typically, the configurational energy, pressure, and N for each counterion are calculated as ensemble averages during the course of the GCMC simulations. In addition, the size of the box (L) has been calculated during the run.

The fraction of counterions ($\alpha_{frac}(M^{n+})$) in EDL has been calculated according to the following formula:

$$\alpha_{frac}(M^{n+}) = \frac{\langle N \rangle_{M^{n+} \times n^+}}{(\langle N \rangle_{M^{1+} \times (1+)} + \langle N \rangle_{M^{2+} \times (2+)} + \dots + \langle N \rangle_{M^{n+} \times n^+}} \quad (2.15)$$

where M^{n+} is a cation with valency n and $\langle N \rangle_{M^{n+}}$ is the average number of M^{n+} in the EDL.

The average double layer concentration of a cation with valency n has been calculated according to the definition

$$\langle C_{DL}^{n+} \rangle = \frac{1660.54 \times \langle N \rangle_{M^{n+}}}{L \times L \times W} \quad (\text{In Molarity (M) unit}) \quad (2.16)$$

The concentration of counterion as a function of distance z from the charged surface has been calculated according to the following equation:

$$C(z) = \langle C_{DL}^{n+} \rangle g(z)$$

The ion exchange or competition has been defined as a ‘‘retention coefficient, γ ’’ where

$$\gamma = \frac{\langle C_{DL}^{n+} \rangle}{C_B^{n+}} \quad (2.17)$$

γ is essentially proportional to ‘‘distribution coefficient, K_d ’’. The retention coefficient γ , has the advantage of being dimensionless. During this work, Xmgrace, 2D graph plotting tool, has been used to illustrate the data.

Chapter Three

Results and Discussion

Throughout this work, a double layer system is considered in equilibrium with a bulk solution that contains a prescribed concentration of the various mono-, di-, tri- and tetravalent cations in addition to a neutralizing monovalent anion. Mono- and divalent cations are sometimes referred to as Na^+ and Ca^{2+} , respectively. The surface charge density is assumed to be negative and of a magnitude corresponding to the clay and cementitious materials, and the separation between the two plates is 3 nm in all simulations. Series of simulations have been performed with systematic variations of different parameters in order to investigate the sorption behavior of the system. The studied parameters include concentration of multivalent ion in the bulk solution, surface charge density of the plates, valency of radionuclides, temperature of the system and ionic strength. In this chapter the retention of trivalent (M^{3+}) and tetravalent (M^{4+}) radioactive ions from bulk solution including 100 mM NaCl and 10 mM CaCl_2 , represents the seawater, by bentonite was studied in section 1. The retention of M^{3+} and M^{4+} ions from different types of water at which the concentration of CaCl_2 is varied was studied in section 2. Finally, the retention of M^{3+} and M^{4+} ions from different types of water at which the concentration of NaCl is varied was studied in section 3.

3.1 Bulk Solution Including 100 mM NaCl, 10 mM CaCl_2 and Radionuclides

A bulk solution that contains 100 mM NaCl, 10 mM CaCl_2 and a prescribed concentration of tri- and tetravalent cations which is in

equilibrium with double layer is constructed. This construction was used in order to investigate the fraction of counterions as a function of multivalent cation concentration in the bulk (section 3.1.1), the average double layer concentration of the multivalent cation and its retention coefficient as a function of multivalent cation bulk concentration (section 3.1.2), surface charge density of plates (section 3.1.3) and temperature of the system (section 3.1.4).

3.1.1 Fraction of Different Counterions in EDL

The fraction of different counterions in the water slit as a function of the concentration of the multivalent ions in the bulk solution has been studied at different surface charge densities (σ) and at room temperature of 298 K. The concentration of trivalent (M^{3+}) and tetravalent (M^{4+}) ions is varied between 10^{-8} to 10^{-3} M. The results are summarized in Figures 3.1. Figure 3.1a shows that the fraction of trivalent cation on electrical double layer increases when its concentration in the bulk is increased. At the same time, the fraction of Ca^{2+} and Na^+ ions decrease, indicating the replacement of Ca^{2+} and Na^+ ions by the trivalent ions in EDL, and this represents the ion exchange reaction. Figure 3.1b shows that the increase of tetravalent ion fraction in EDL as a result of increasing its concentration in the bulk is also accompanied by a decrease in the fraction of Ca^{2+} and Na^+ ions in EDL. It is clear from figure 3.1 that the increase of the fraction of multivalent cation is faster for higher surface charge density of the plates. At specific bulk concentration of the multivalent cation, for example, 10^{-5} M of tetravalent cation with $\sigma = -0.7, -2, -3$ e/nm² the fractions are 0.13, 0.8, 0.92, respectively.

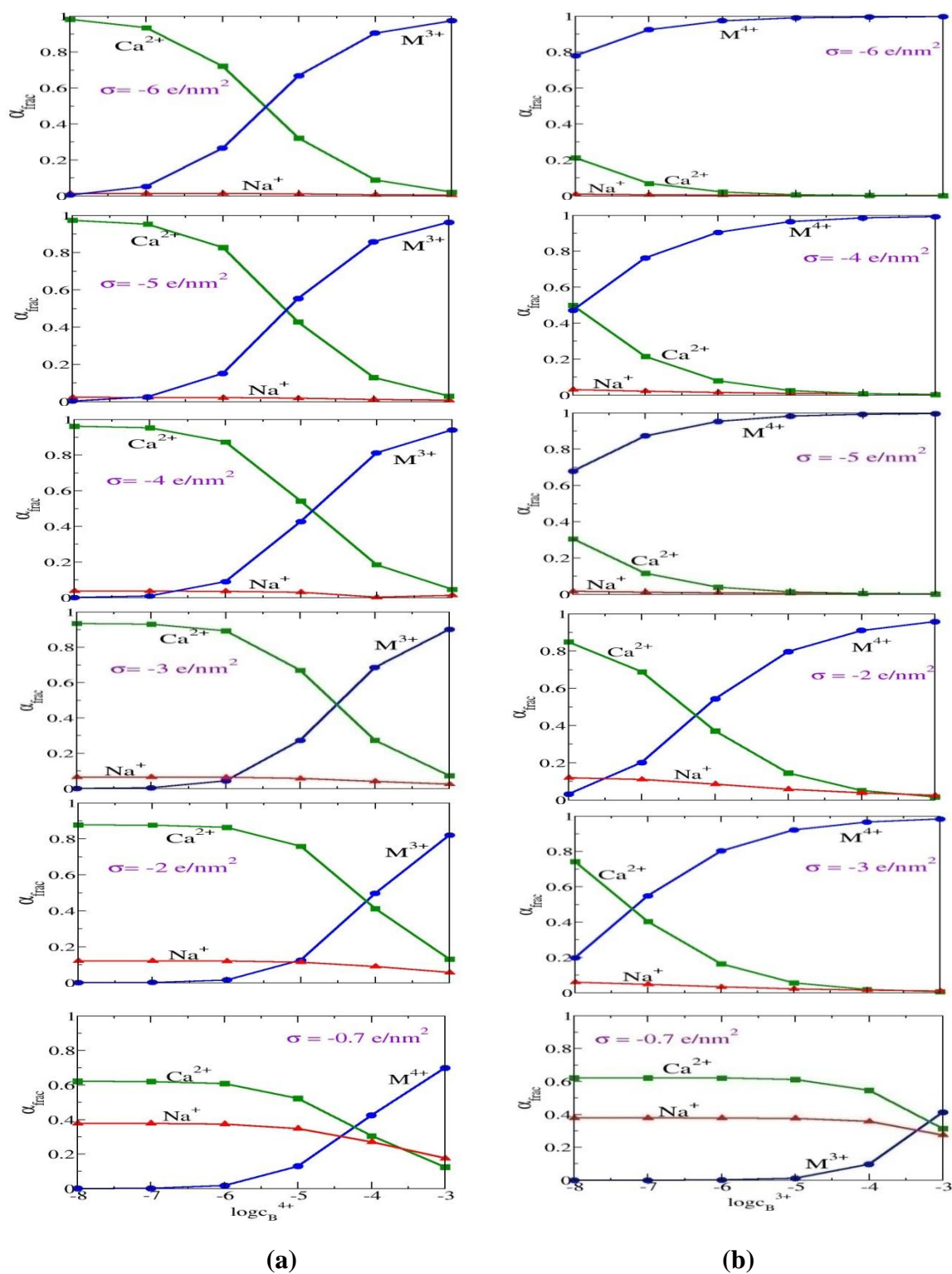


Figure 3.1: Fraction of different counterions in the slit as a function of a) trivalent and b) tetravalent cations concentration in the bulk. The surface charge density has been varied. The slit in equilibrium with a bulk containing 100 mM NaCl, 10 mM CaCl₂ and varying amount of multivalent cations. The slit width is 3 nm.

Note that at a certain concentration the multivalent ions will start to dominate the electrical double layer. Figure 3.1a shows that at $\sigma = -0.7, -2, -3 \text{ e/nm}^2$, the domination of electrical double layer by trivalent cation starts at $10^{-3}, 10^{-4}$ and 10^{-5} M , respectively. On the other hand, for tetravalent (Figure 3.1b), the concentration $10^{-4}, 10^{-6}, 10^{-7} \text{ M}$ is enough to start to dominate the double layer at $\sigma = -0.7, -2, -3 \text{ e/nm}^2$, respectively. It is interesting to note that by increasing the surface charge density the domination of the multivalent cation occurs at lower concentration.

The trivalent cation will be more abundant in the double layer at higher surface charge densities i.e. $-4, -5, -6 \text{ e/nm}^2$ and will dominate the EDL at lower concentration. The tetravalent cation, on the other hand, dominates the EDL at all the concentration scale with surface charge densities above -4 e/nm^2 . In addition, at higher concentration the fraction of tetravalent cation is unity which means that it completely neutralized the charged surface.

3.1.2 Effect of Multivalent Cations Concentration in the Bulk Solution

The sorption of multivalent cation on bentonite as a function of their concentration in the bulk was studied at different surface charge densities by varying the multivalent cation bulk concentration from 10^{-8} to 10^{-3} M at 298 K. The slit is in equilibrium with a bulk containing 100 mM NaCl, 10 mM CaCl_2 (seawater) and varying amount of multivalent cations. Figure 3.2a indicates that the average double layer concentration of trivalent cation increases by increasing its concentration in the bulk.

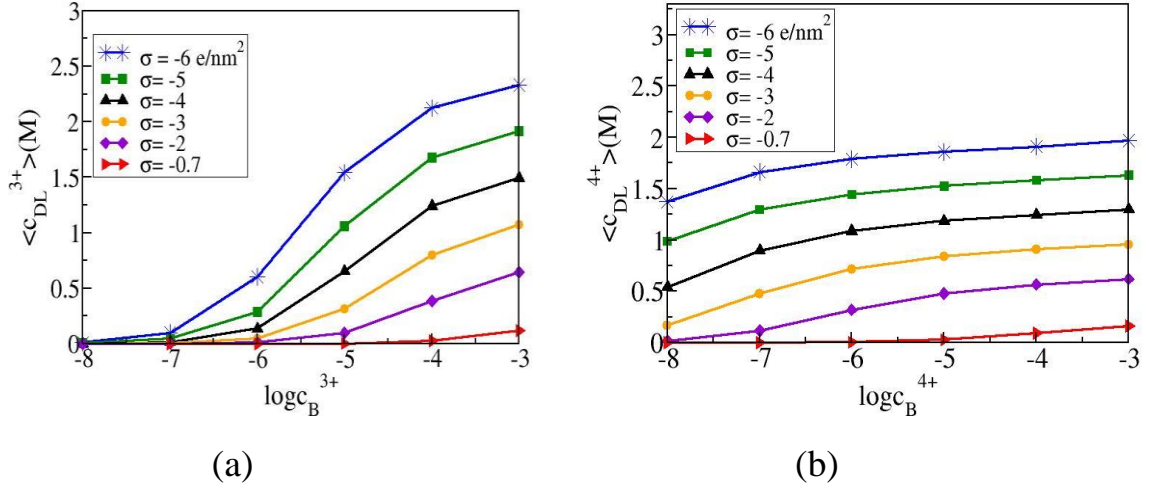


Figure 3.2: Average double layer concentration of a) trivalent and b) tetravalent cations as a function of their bulk concentrations. The surface charge density has been varied. The bulk contains 100 mM of NaCl and 10 mM of CaCl₂.

Figure 3.2b shows that the average double layer concentration of tetravalent cation especially at higher surface charge densities increases by increasing its concentration in the bulk solution until the double layer is completely neutralized by the cation. So, anymore increase of the tetravalent cation concentration in the bulk will not change $\langle c_{DL}^{4+} \rangle$.

The spatial distribution of counterions in EDL was studied as a function of distance (z) from the charged surface for two different bulk concentrations of multivalent cations 0.01 mM (figure 3.3a) and 0.1 mM (figure 3.3b). The surface charge density of the plates is -2 e/nm².

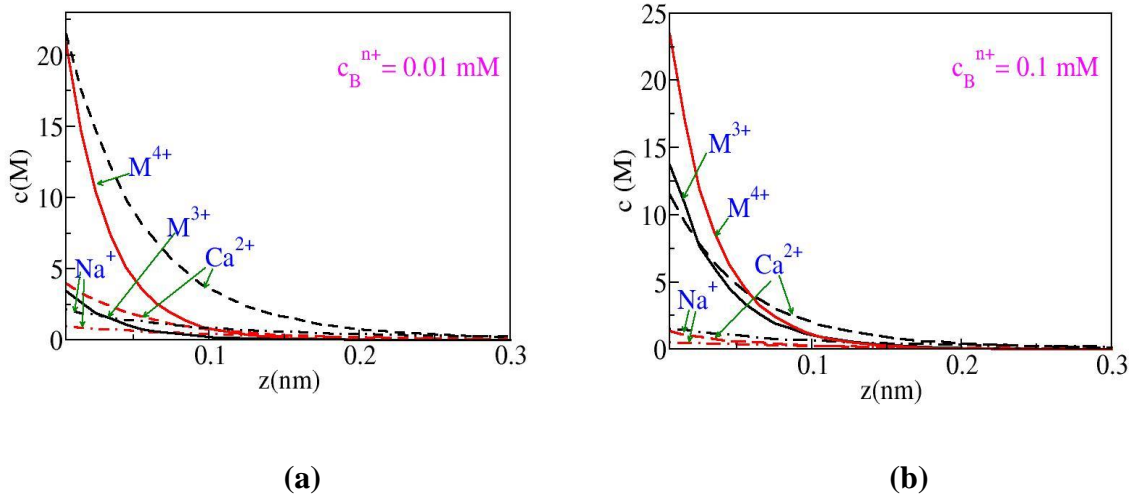


Figure 3.3: Concentration of counterions as a function of distance from the charged surface. Two different bulk systems are shown with 100 mM Na^+ , 10 mM of Ca^{2+} and a) 0.01 mM of M^{n+} ions b) 0.1 mM of M^{n+} ions. The slit width is 3 nm and the surface charge density is -2 e/nm^2 . Trivalent system (black curves) and tetravalent system (red curves).

By looking at figure 3.3a at which the two bulk systems have 0.01 mM of multivalent cations, it is clear that the distribution of tetravalent species is completely dominated over divalent one in EDL, while divalent distribution is dominated over trivalent on the other bulk system. By increasing the bulk concentration for multivalent cation to 0.1mM as in figure 3.3b it is noted that the concentration of trivalent cation increases and the concentration of Ca^{2+} decreases until the distribution of trivalent and divalent cations are rather similar. However, the concentration of tetravalent cation increases and it is still the dominant.

Figure 3.4 shows the spatial distribution of tetravalent cation in electrical double layer in contact with a bulk. The bulk contains 100 mM NaCl , 10 mM CaCl_2 and a varying amount of tetravalent cations, this figure illustrates how the double layer becomes saturated with tetravalent species. That is, a change from 0.00001 to 0.0001 mM and from 0.0001 to 0.001

mM in the bulk concentration of tetravalent cation has a significant effect on the double layer content of M^{4+} , while a further increase only leads to marginal increase of the concentration in the double layer. So, it is clear from the figure that the double layer is saturated by tetravalent cation nearly at 0.01mM.

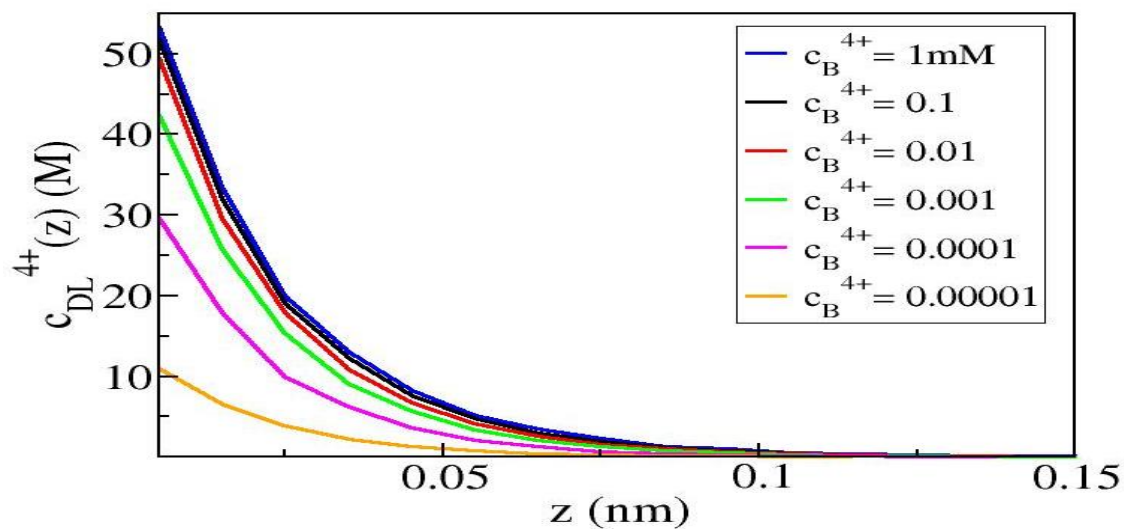


Figure 3.4: Concentration of tetravalent cations as a function of distance from the charged surface. The surface charge density is -3 e/nm^2 and the bulk solution contains 100 mM of NaCl, 10 mM of CaCl_2 and varying amount of tetravalent cations as indicated in the graph. The slit width is 3 nm.

The retention coefficient, represented by $\gamma = \frac{\langle c_{DL} \rangle^{n+}}{c_B^{n+}}$, as a function of multivalent cation bulk concentration is shown in figure 3.5. Figure 3.5a shows that the retention coefficient for trivalent cation approaches a constant value at low concentrations then it decreases linearly at higher ones, as at higher concentrations a marginal increase in double layer concentration of trivalent cation is recorded (figure 3.2a).

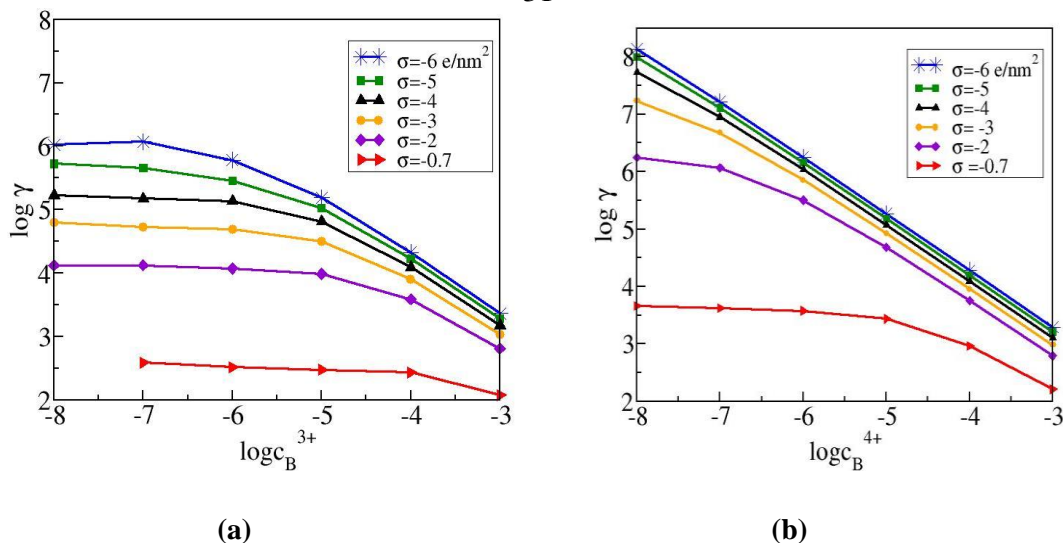


Figure 3.5: The retention coefficient of a) trivalent and b) tetravalent cations as a function of the bulk concentrations. The surface charge density has been varied. The bulk also contains 100 mM of NaCl and 10 mM of CaCl₂.

In figure 3.5b, it is clear that at low surface charge density ($\sigma = -0.7 \text{ e/nm}^2$) the retention coefficient of tetravalent cation is almost constant between 10^{-8} to 10^{-5} M , then it decreases sharply. Also, at $\sigma = -3 \text{ e/nm}^2$, the retention coefficient decreases sharply after 10^{-6} M since any further increase only leads to marginal increase of the concentration in the double layer (figure 3.4). However at higher values of surface charge densities i.e. -4, -5, -6 e/nm^2 the retention coefficient decreases sharply by increasing the bulk concentration of tetravalent cation.

These results are similar to those previously reported for the sorption of various metal ions on a variety of sorbents (Khan *et al.*, 1995). In that experiment, the Cr(III) distribution coefficient was found to decrease by increasing its concentration in the solution.

3.1.3 Effect of Surface Charge Density

The effect of changing surface charge density of the plates on the sorption of multivalent cation on bentonite was studied by varying the surface charge density from -0.7 to -11 e/nm^2 for trivalent cation system and to -13 e/nm^2 for tetravalent system at 298 K . The slit is in equilibrium with a bulk that contains 100 mM NaCl , 10 mM CaCl_2 (seawater) and constant amount of multivalent cation. The results of simulations are shown in figure 3.6.

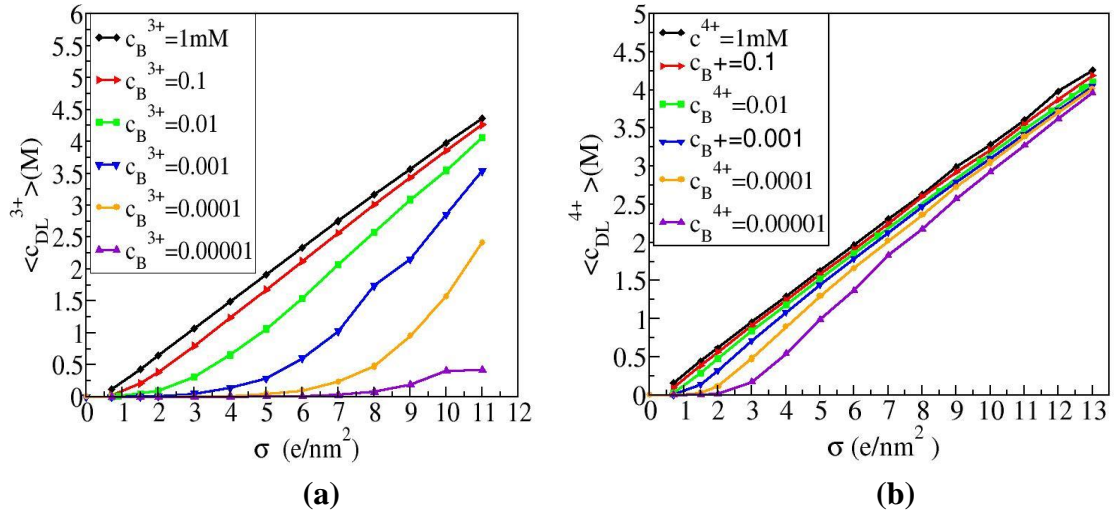


Figure 3.6: Average double layer concentration of a) trivalent and b) tetravalent cations as a function of surface charge density of the walls. The bulk contains 100 mM of NaCl and 10 mM of CaCl_2 and varied concentration of the multivalent cations.

The sorption data of the tetravalent cation seemed to lead to a linear behavior as a function of surface charge density for almost all shown bulk concentration (figure 3.6b). While the sorption of trivalent cation leads to be linear at higher bulk concentration (figure 3.6a). Because by increasing the surface charge density more and more cations are needed to neutralize the surface charge.

The spatial distribution of counterions in EDL was studied as a function of distance (z) from the charged surface for surface charge densities -2 e/nm^2 (figure 3.7a) and -3 e/nm^2 (figure 3.7b). It is noted that, by increasing surface charge density to -3 e/nm^2 the concentration of each ion in EDL increases, so, the capacity of EDL increases.

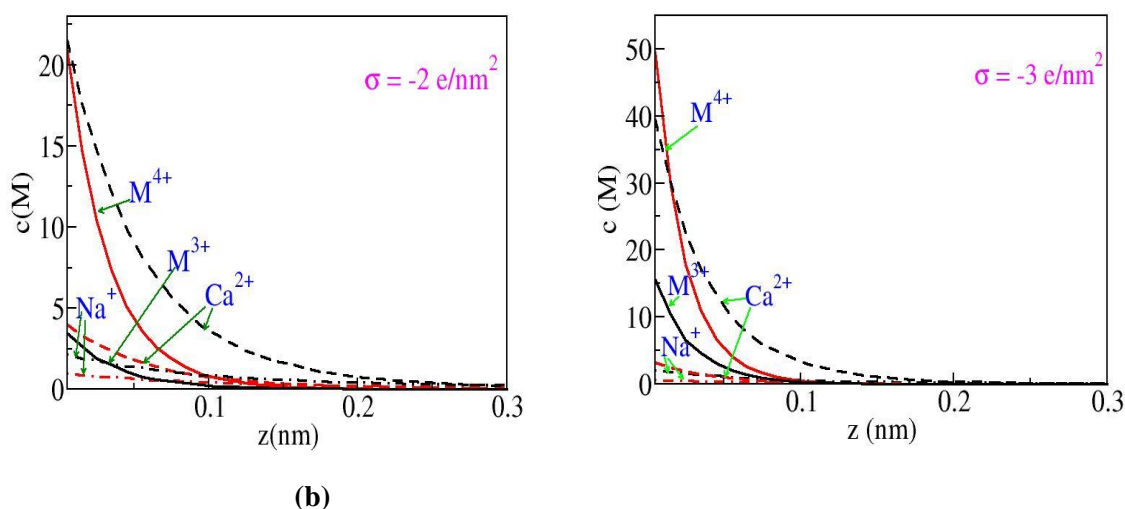


Figure 3.7: Concentration of counterions as a function of distance from the charged surface. Two different bulk systems are shown with 100 mM Na^+ , 10 mM of Ca^{2+} and 0.01 mM of M^{n+} ions, at surface charge density of a) -2 e/nm^2 b) -3 e/nm^2 . Trivalent system (black curves) and tetravalent system (red curves).

Figure 3.8 shows the retention coefficient of the multivalent ions as a function of surface charge density. It is clear that the retention coefficient is increased by increasing surface charge density at specific bulk concentration. Really, there is a relation between the surface charge density of the plates and the pH of the solution. The concentrations of the surface groups of the montmorillonite change at different pH values. In alkaline solutions, the surface hydroxyl groups can dissociate $\text{DOH} \leftrightarrow \text{DO}^- + \text{H}^+$. So, with increasing pH, the number of negatively surface charged groups

(DO^-) increases and this means that the total negative surface charge density of the clay increases. There is some agreement between these predictions about the sorption behavior of multivalent ion as a function of pH of the solution and experimental investigations. Cr(III) (Khan *et al.*, 1995), As(III) (Manning *et al.*, 1996), Am(III) (Yu *et al.*, 2012), Bi(III) (Ulrich and Degueldre, 1993) Eu(III) (Songsheng *et al.*, 2012) and Th(IV) (Zhao *et al.*, 2008) distribution coefficients increases by increasing pH of the solution.

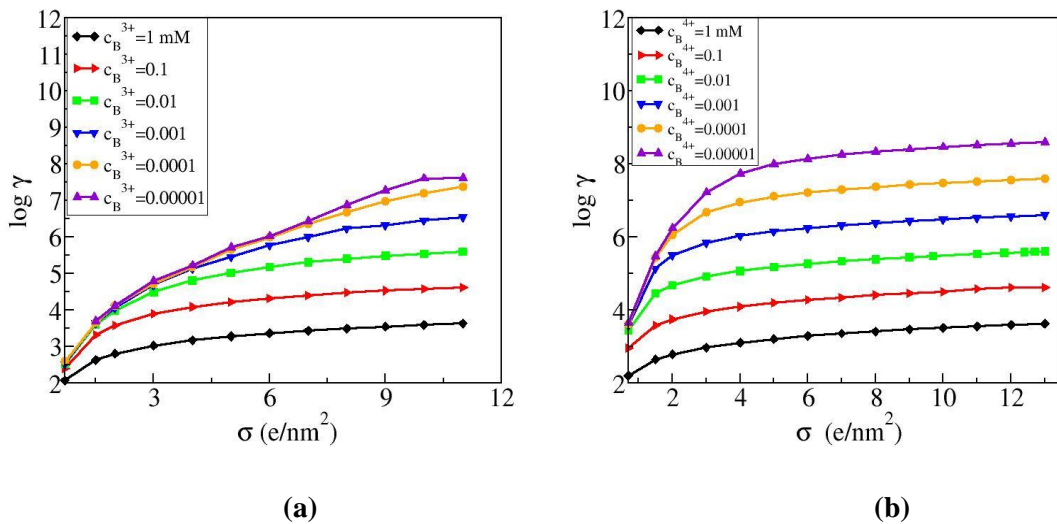
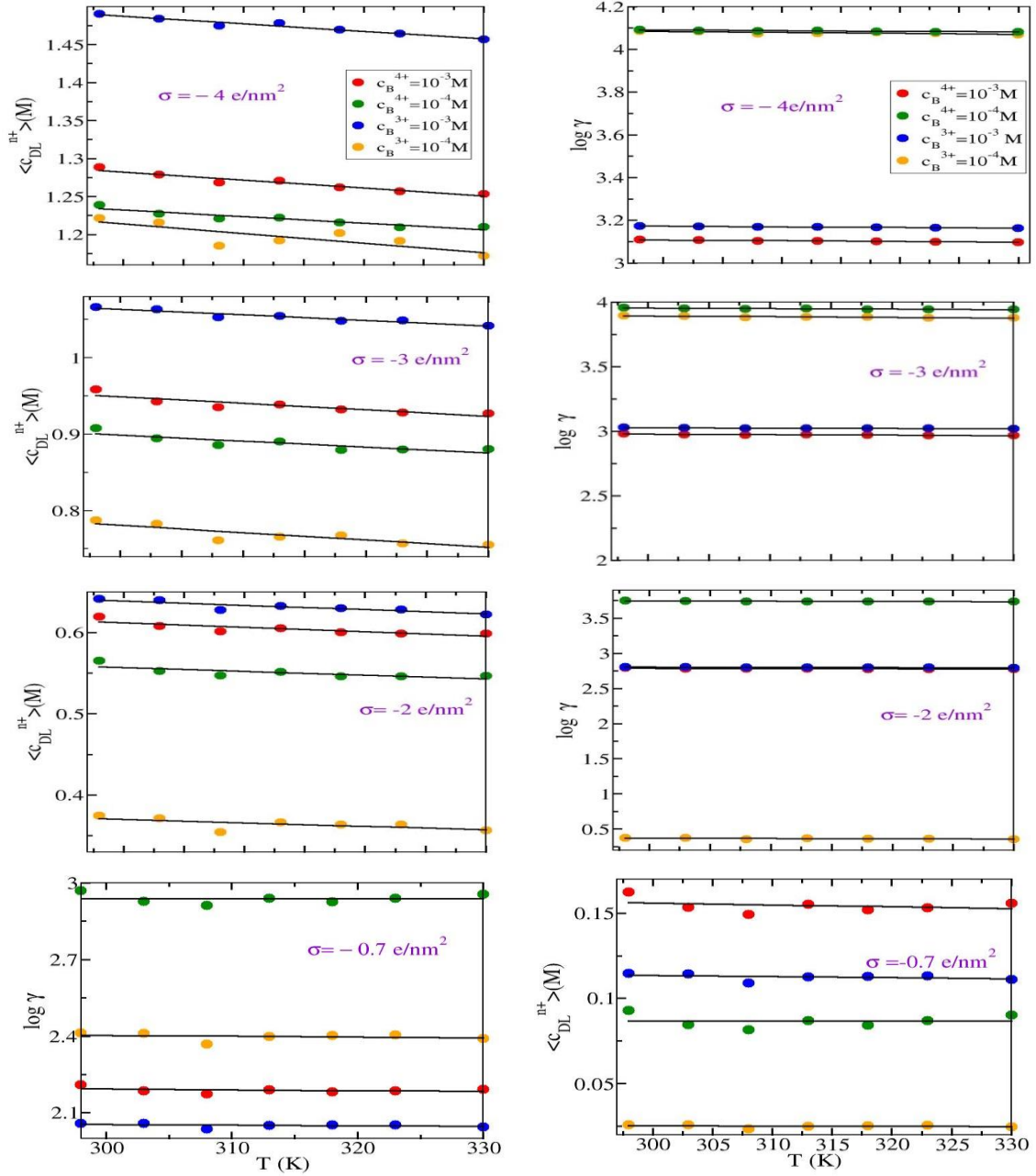


Figure 3.8: The retention of a) trivalent and b) tetravalent cations as a function of surface charge density of the walls. The bulk contains 100 mM of NaCl and 10 mM of CaCl_2 and varied concentration of the multivalent cations.

3.1.4 Effect of Temperature

The dependence of multivalent ion sorption on temperature was studied at surface charge densities by varying the temperature of the system from 298 to 330 K. The slit is in equilibrium with a bulk containing 100 mM NaCl, 10 mM CaCl_2 (seawater) and constant amount of multivalent cation.



(a)

(b)

Figure 3.9: a) Average double layer concentration of multivalent cations as a function of temperature at different values of surface charge densities. The slit in equilibrium with a bulk containing 100 mM NaCl, 10 mM CaCl₂ and constant amount of multivalent cation. b) The retention coefficient of tri- and tetravalent cations as a function of temperature calculated from curves in figure 3.9a. Dots are the simulation results while the solid lines are liner fit.

The simulation results shown in figure 3.9a indicate that the sorption is less favored at high temperatures. For the physical adsorption of multivalent ions on clay the attraction between the cations and the surface is almost the exclusive driving force. Thermodynamically this means that such cations adsorption is exothermic, so, the sorption process is spontaneous and this could explain the decreasing behavior.

Figure 3.9b shows the retention coefficient of tri- and tetravalent cations as a function of temperature. It is obvious that the retention coefficient decreases very slowly by increasing temperature since a marginal decrease was registered in double layer concentration. By returning to previous studies one can note that the sorption of Cr(III) (Khan *et al.*, 1995) and Th(IV) (Zhao *et al.*, 2008) inhibits by increasing temperature.

3.2 Bulk Solution Including 100 mM NaCl, x mM CaCl₂ and Radionuclides

In this section the sorption of tri- and tetravalent cations from other waters is investigated. In such waters, the concentration of NaCl was 100 mM while the concentration of CaCl₂ was varied. The fraction of different counterions was found as a function of multivalent cation bulk concentration at three different bulk solutions. The average double layer concentration of multivalent cations was studied as a function of different systems of water.

The fraction of different counterions in EDL has been studied as a function of multivalent bulk concentration at different bulk solutions; 100 mM NaCl + 50 mM CaCl₂, 100 mM NaCl + 100 mM CaCl₂, 100 mM NaCl + 300 mM CaCl₂. The surface charge density was kept constant at -3 e/nm^2 . The simulations were done at constant temperature 298 K. The results of

simulations are shown in figure 3.10. Figure 3.10a shows that the fraction of trivalent cation in EDL at lower concentration of it in the bulk is nearly zero. On the other hand, divalent cation is the dominant. While trivalent cation is more abundant in a slit with equilibrium with the bulk solution containing lower CaCl_2 concentration.

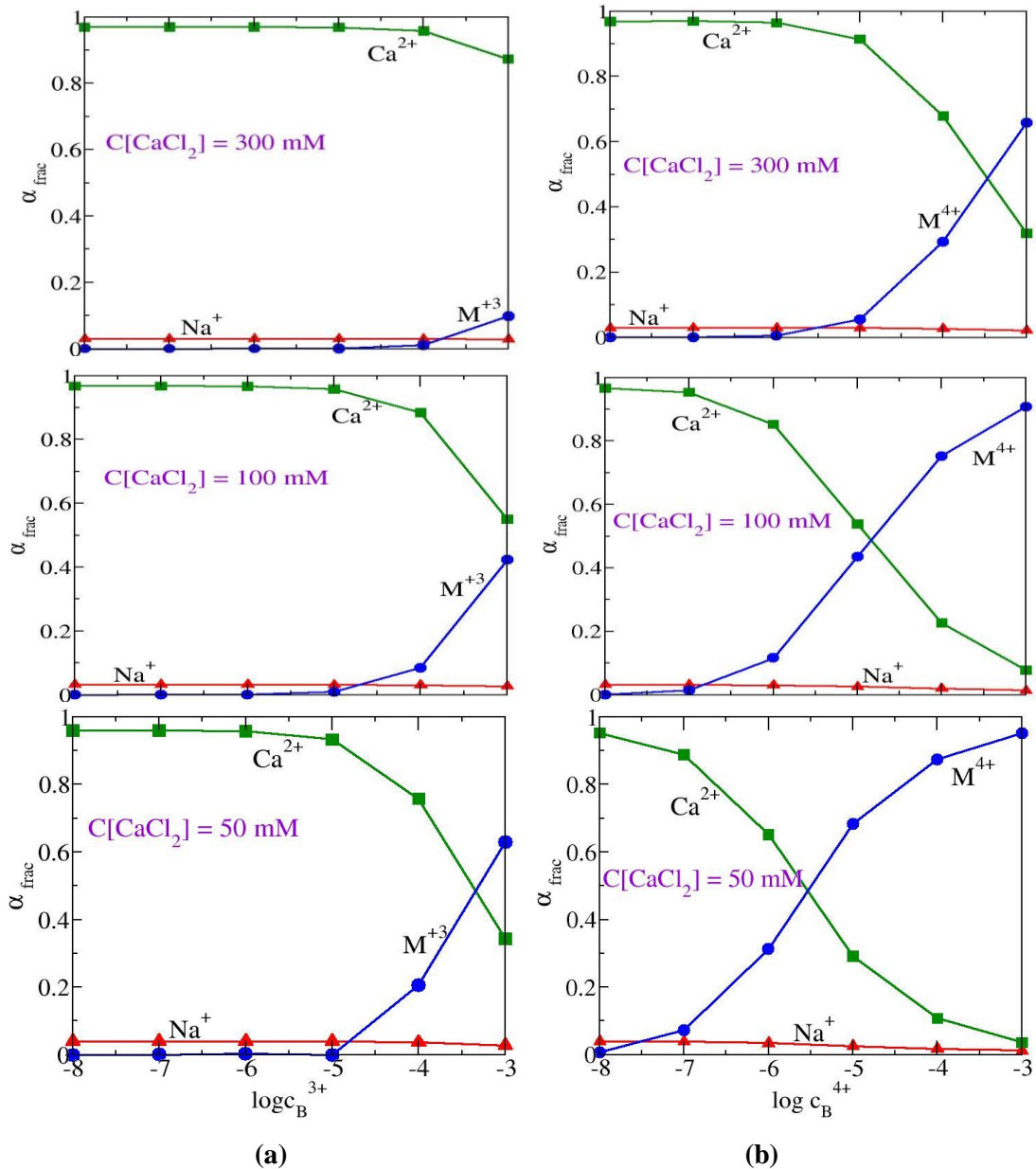


Figure 3.10: Fraction of different counterions in the slit as a function of a) trivalent b) tetravalent cations concentration at different bulk solution; 100 mM NaCl + 50 mM CaCl_2 , 100 mM NaCl + 100 mM CaCl_2 and 100 mM NaCl + 300 mM CaCl_2 . The surface charge density is -3 e/nm^2 and the slit width is 3nm.

As shown in figure 3.10b, the fraction of tetravalent cation in EDL decreases by increasing the concentration of CaCl_2 in the bulk solution, while the fraction of Ca^{2+} increases and the fraction of Na^+ remains constant.

The sorption of tri- and tetravalent cations on bentonite has been studied as a function of CaCl_2 concentration by varying the bulk concentration of CaCl_2 from 10 to 500 mM. The slit is in equilibrium with a bulk contains 100 mM NaCl, 1mM of multivalent cation and varying amount of CaCl_2 at different surface charge densities. The influence of CaCl_2 on the adsorption of multivalent cation on bentonite is represented in figure 3.11a. The results indicate that by increasing the concentration of CaCl_2 in the bulk will inhibit the sorption of multivalent cation in electrical double layer. This behavior can be explained by the adsorption of multivalent ions by electrical forces, then the presence of competing cations of the salt will reduce the adsorption. It is interesting to note that changing ionic strength of the bulk system has more effect on trivalent cation adsorption than tetravalent one.

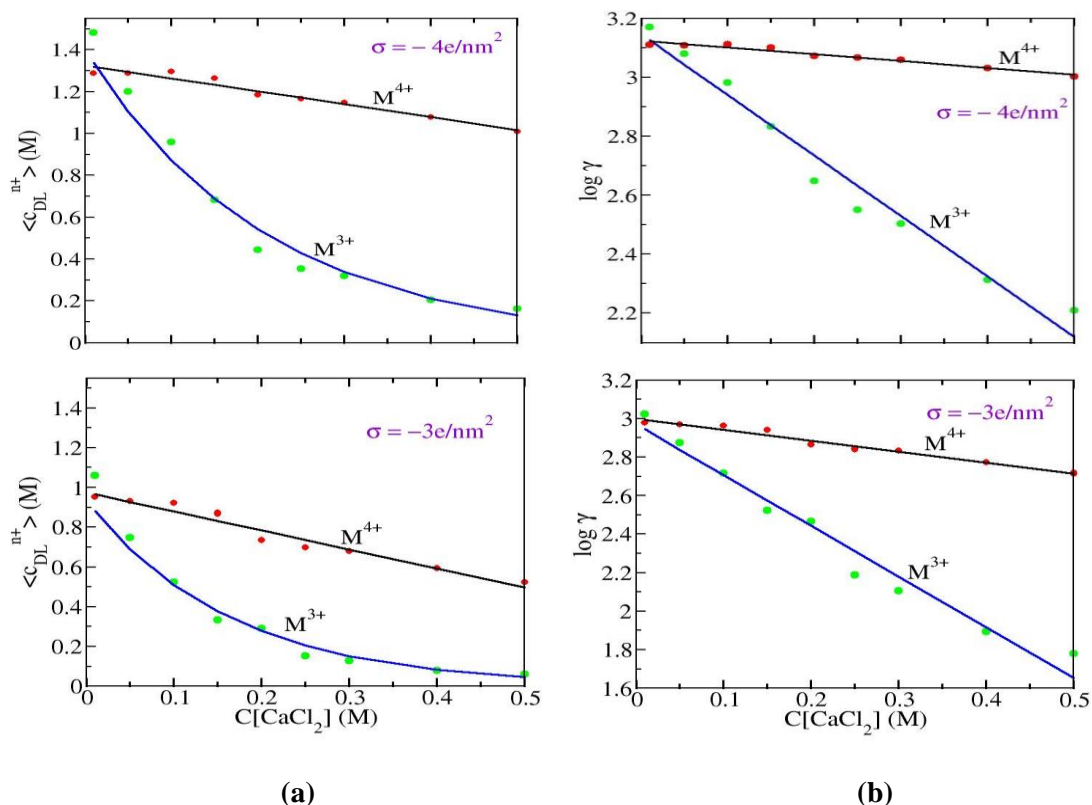


Figure 3.11: a) Average double layer concentration of multivalent cation as a function of $CaCl_2$ concentration at two different surface charge densities. The bulk contains 100 mM NaCl, 1 mM of multivalent cations and a varying amount of $CaCl_2$. b) The retention coefficient as a function of $CaCl_2$ concentration calculated from the curves in figure 3.11a. Dots are the simulation results while the solid lines are linear fit or exponential fit.

The retention coefficient as a function of $CaCl_2$ concentration is shown in figure 3.11b. It is obvious that the retention coefficient is decreased by increasing $CaCl_2$ concentration. This is in agreement with previous studies (Sabodina *et al.*, 2006, Zhao *et al.*, 2008, Yu *et al.*, 2012) which show that the adsorption of multivalent ions is decreased with increasing ionic strength.

The average double layer concentration of tri- (3.12a) and tetravalent (3.12b) cations as a function of its concentration in the bulk solution at different bulk solutions is shown in figure 3.12. The surface charge density

was -3 e/nm^2 . It is obvious that the sorption of multivalent ion from the solution that contains 50 mM CaCl_2 is more effective than the sorption from the other solutions.

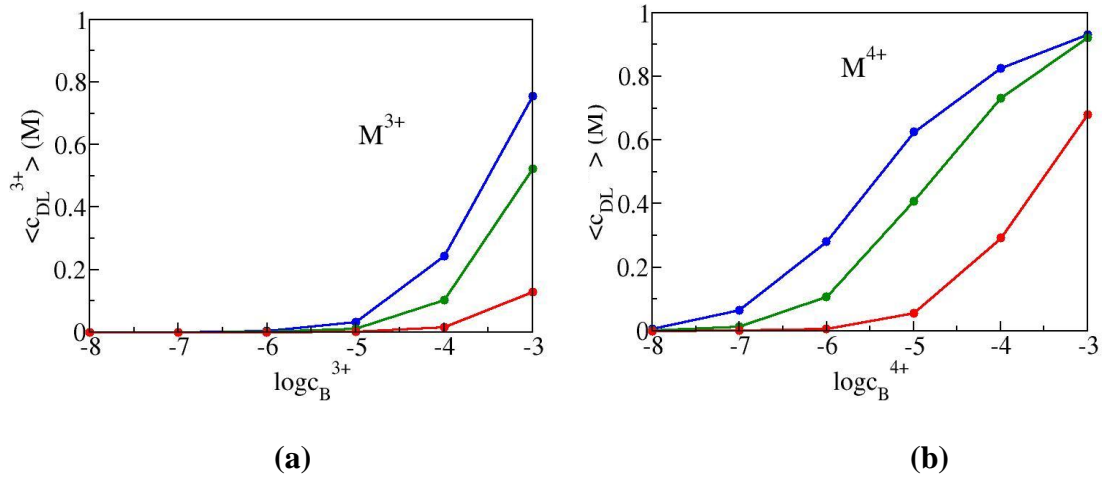


Figure 3.12: Average double layer concentration of a) trivalent and b) tetravalent cations as a function of multivalent cations concentration in the bulk. The surface charge density was -3 e/nm^2 . The bulk condition was varied: blue lines = $100 \text{ mM NaCl} + 50 \text{ mM CaCl}_2$, green lines = $100 \text{ mM NaCl} + 100 \text{ mM CaCl}_2$ and red lines = $100 \text{ mM NaCl} + 300 \text{ mM CaCl}_2$. The slit width is 3 nm .

3.3 Bulk Solution Including $x \text{ mM NaCl}$, 10 mM CaCl_2 , and Radionuclides

Further simulation were performed for studying the sorption of multivalent cations from other waters in which CaCl_2 concentration was 10 mM while the concentration of NaCl was varied. The fraction of different counterions was found as a function of multivalent cation bulk concentration at three different bulk solutions. The Average double layer concentration of multivalent was studied as a function of different systems of water.

The fraction of different counterions in EDL has been studied as a function of multivalent bulk concentration at different bulk solutions; 200 mM NaCl

+ 10 mM CaCl_2 , 400 mM NaCl + 10 mM CaCl_2 , 500 mM NaCl + 10 mM CaCl_2 (ocean water). The surface charge density was kept constant at -3 e/nm^2 . The simulations were done at constant temperature 298 K. The results of simulations are shown in figure 3.13. Figure 3.13a shows that by increasing the trivalent concentration in the bulk the fraction of it in EDL increases at different bulk solutions while the fraction of Ca^{2+} and Na^+ decreases. Moreover, the trivalent cation is more abundant in the solution having lower NaCl concentration. It is clear that an increase in NaCl concentration in the bulk leads to a decrease in the fraction of Ca^{+2} and increase in the fraction of Na^+ . On the other hand, it is obvious that the fraction of tetravalent cation decreases by increasing the NaCl concentration as shown in figure 3.13b.

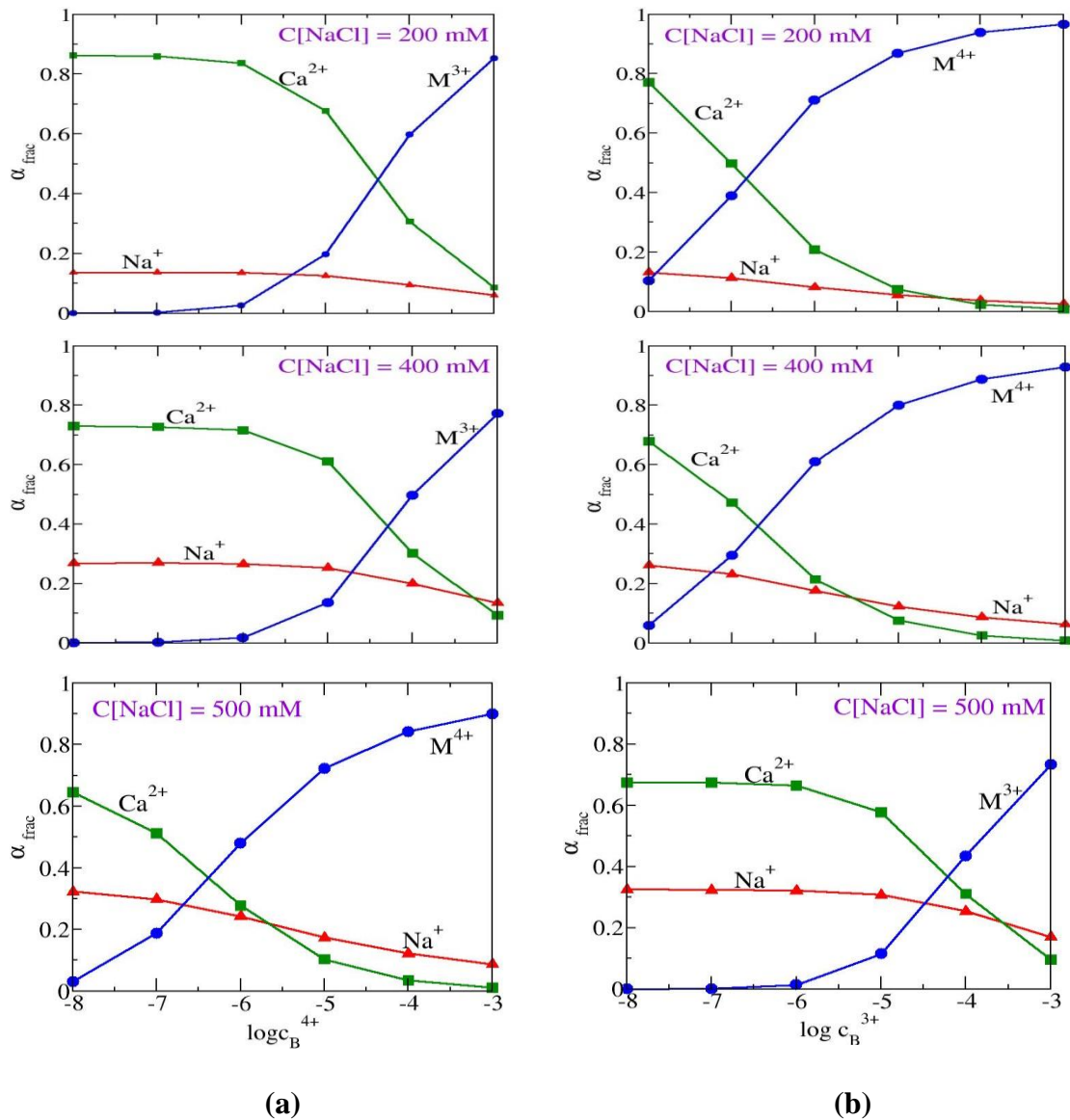


Figure 3.13: Fraction of different counterions in the slit as a function of a) trivalent b) tetravalent cations concentration at different bulk solutions; 200 mM NaCl + 10 mM CaCl_2 , 400 mM NaCl + 10 mM CaCl_2 and 500 mM NaCl + 10 mM CaCl_2 . The surface charge density has been kept constant at -3 e/nm^2 . The slit width is 3nm.

The effect of changing NaCl concentration in the bulk system on the sorption of multivalent cation was also studied by varying the bulk concentration of NaCl from 50 to 500 mM. The slit is in equilibrium with a bulk containing 10 mM CaCl_2 , 0.001 mM of multivalent cation and varying

amount of NaCl at surface charge density of -3 e/nm^2 . The average double layer concentration of tri- and tetravalent cations decreases by increasing the concentration of NaCl as shown in figure 3.14a.

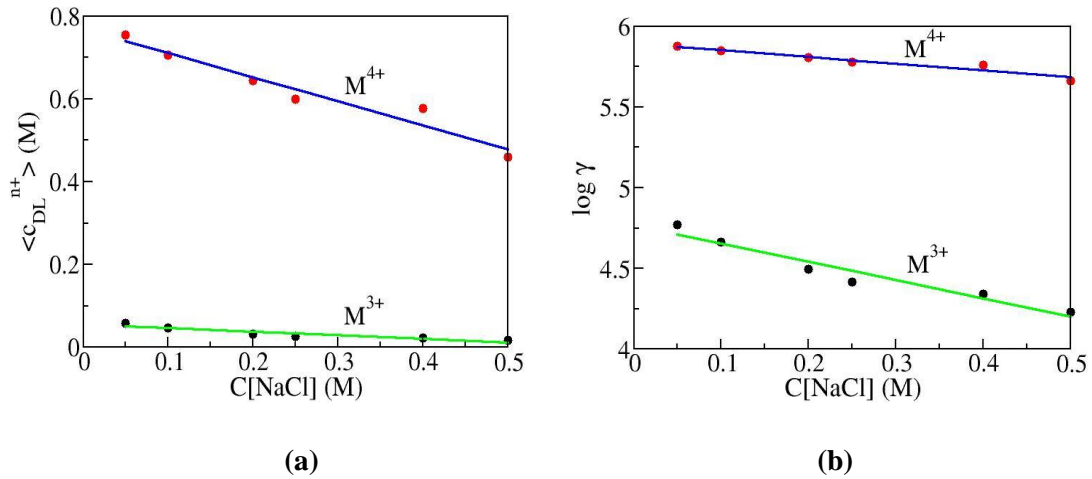


Figure 3.14: a) Average double concentration of trivalent cation (black symbol) and tetravalent cation (red symbol) as a function of NaCl concentration. Bulk solution contains 10 mM CaCl_2 , 0.001 mM of multivalent cations. Surface charge density = -3 e/nm^2 b) The retention coefficient calculated from curves in figure 3.14a. Dots are the simulation results while the solid lines are liner fit.

Moreover, the effect of monovalent cations on the retention coefficient of tri- and tetravalent pollutants is demonstrated in figure 3.14b. It is obvious that the retention coefficient of cations is decreased by increasing NaCl concentration. This is in agreement with some experimental previous studies (Yu *et al.*, 2012) in which the adsorption of Am(III) ions is decreased with increasing NaCl concentration.

Further simulations have been performed for studying the effect of changing the multivalent bulk concentration on the average double layer concentration of the multivalent cations at three bulk solutions; 200 mM NaCl +10 CaCl_2 , 400 mM NaCl +10 mM CaCl_2 and 500 mM NaCl + 10

mM CaCl_2 . The surface charge density was -3 e/nm^2 . The results are shown in figure 3.15 which reveals that the sorption of multivalent pollutants is stronger in less salted bulk solution.

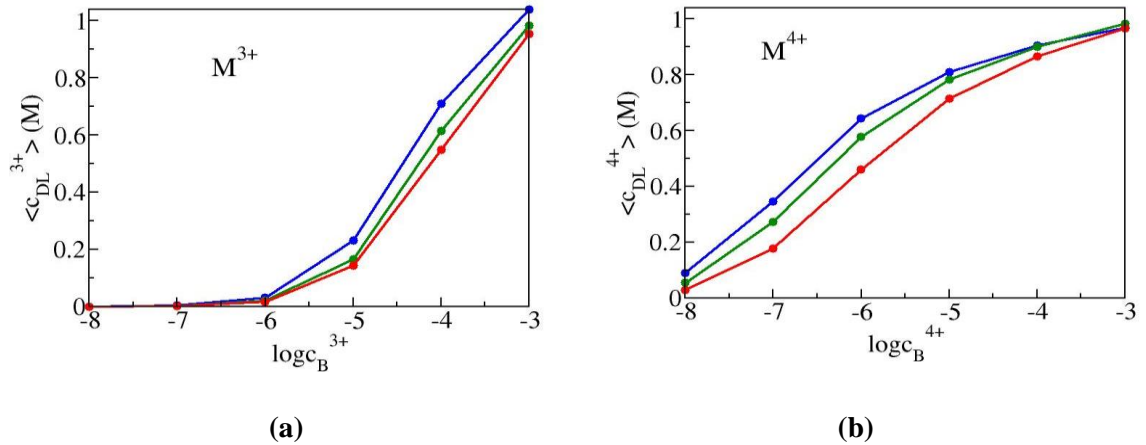


Figure 3.15: Average double layer concentration of a) trivalent and b) tetravalent cations as a function of their concentration in the bulk. The surface charge density has been kept constant at -3 e/nm^2 and the slit width is 3 nm. The bulk condition has been varied: blue lines = 200 mM NaCl + 10 mM CaCl_2 , green lines = 400 mM NaCl + 10 mM CaCl_2 and red lines = 500 mM NaCl + 10 mM CaCl_2 . The slit width is 3nm.

For comparison another series of simulations have been done in order to demonstrate the effect of mono- and divalent cations on the retention of multivalent (M^{3+} , M^{4+}) pollutants at $\sigma = -4 \text{ e/nm}^2$ and 1mM of multivalent cation. As can be seen in figure 3.16, the retention coefficient of multivalent cation is weakly affected by NaCl concentration while strongly by CaCl_2 concentration.

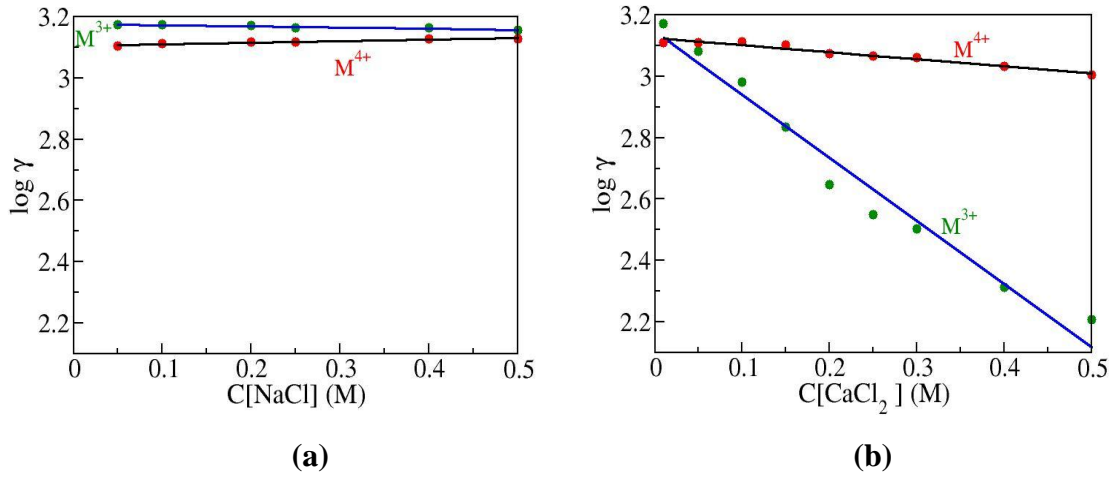


Figure 3.16: Retention coefficient of multivalent cation as a function of a) NaCl concentration, the bulk solution contains 10 mM CaCl_2 1mM of multivalent cations and a varying amount of NaCl b) CaCl_2 concentration, the bulk contains 100 mM NaCl, 1 mM of multivalent cations and a varying amount of CaCl_2 . The surface charge density is $-4 e/\text{nm}^2$. The slit width is 3nm. Dots are the simulation results while the solid lines are linear fit.

Chapter Four

Conclusions

The retention of tri- and tetravalent radionuclides has been studied using Grand Canonical Monte Carlo simulation. Based on the findings of these studies, the following main conclusions can be obtained:

- ❖ The interplay of coulomb interactions allows us to explain the adsorption of multivalent pollutants.
- ❖ There exists a strong competition between the counterions of different valencies which means that a relatively small concentration of multivalent counterions in the bulk is enough to have a double layer that is completely dominated by the multivalent ions.
- ❖ The outcome of the competition of counterions of different valencies depends on several factors: the valency of counterion M , surface charge density, temperature of the bulk, as well as the bulk concentration of all charged species.
- ❖ The fraction of trivalent and tetravalent cation on electrical double layer increases when its concentration in the bulk is increased. At the same time the fraction of Ca^{2+} and Na^+ ions decreases. However, this fraction decreases by increasing the concentration of CaCl_2 or NaCl in the bulk solution.
- ❖ The retention coefficient of multivalent cation is weakly affected by NaCl concentration while strongly affected by CaCl_2 concentration.

- ❖ The retention coefficient of multivalent cationic pollutants (M^{3+} and M^{4+}) increases by increasing the surface charge density of the plates.
- ❖ The retention coefficient of multivalent cationic pollutants (M^{3+} and M^{4+}) decreases by increasing:
 - a) the bulk concentration of these pollutants.
 - b) the temperature of the bulk.

References

- Allard, B., Rydberg, J., Kipatsi, H., & Torstenfelt, B. (1979). Disposal of radioactive waste in granitic bedrock. In S. Fried (Ed.), *Radioactive Waste in Geologic Storage* (pp. 47-73). American Chemical Society.
- Allen, M. P., & Tildesley D. J. (1987). *Computer Simulation of Liquid*, Oxford: Clarendon Press.
- Bartle, U., & Czurda, K. A. (1991). **Migration and retention phenomena of radionuclides in clay-barrier systems.** *Applied Clay Science*, 6, 195-214.
- Baston, G. M. N., Berry, j. A., Brownsword, M., Cowper, M. M., Heath, T. J., & Tweed, C. J. (1995). **The sorption of uranium and technetium on bentonite, tuff and granodiorite.** *Materials Research Society Symposium Proceedings*, 353, 989-996.
- Benedicto, A., Degueldre, C., & Missana, T. (2014). **Gallium sorption on montmorillonite and illite colloids: Experimental study and modelling by ionic exchange and surface complexation.** *Applied Geochemistry*, 40, 43–50.
- Bradbury, M. H., & Baeyens, B. (1997). **A mechanistic description of Ni and Zn sorption on Na – montmorillonite, Part II: modelling,** *Journal of Contaminant Hydrology*, 27, 223-248.
- Bradbury, M. H., & Baeyens, B. (2005). **Modelling the sorption of Mn(II), Co(II), Ni(II), Zn(II), Cd(II), Eu(III), Am(III), Sn(IV), Th(IV) Np(V) and on montmorillonite: Linear free energy relationships and estimates of surface binding constants for some**

- selected heavy metals and actinides.** *Geochemica et Cosmochimica Acta*, 69(4), 875-892.
- Brémaud, P. (1999). *Markov Chains: Gibbs Fields, Monte Carlo simulation, and Queues*. New York: Springer-Verlag.
 - Debnath, S., & Ghosh, U. C. (2009). **Nanostructured hydrous titanium (IV) oxide: Synthesis, characterization and Ni (II) adsorption behavior.** *Chemical Engineering Journal*, 152, 480-491.
 - Di Natale, F., Erto, A., Lancia, A., & Musmarra, D. (2008). **Experimental and modeling analysis of As (V) ions adsorption on granular activated carbon.** *Water Research*, 42, 2007-2016.
 - Dzombak, D. A., & Hudson, R. J. M. (1995). Ion Exchange The Contributions of Diffuse Layer Sorption and Surface Complexation. In C. P. Huang, C. R. O'Melia, & J. J. Morgan (Eds.), *Aquatic Chemistry: Interfacial and Interspecies Processes* (pp. 59). Washington DC: American Chemical Society.
 - Ángeles, F. J., & Cassou, M. L. (2004). **Simple Model for Semipermeable Membrane: Donnan Equilibrium.** *Journal of Physical Chemistry. B*, 108, 1719-1730.
 - Fletcher, P., & Sposito, G. (1989). **The Chemical Modelling of Clay Electrolyte Interactions for Montmorillonite.** *Clay Minerals*, 24, 375-391.
 - Frenkel, D., & Smit, B. (1996). *Understanding Molecular Simulation. From Algorithms to Applications*. San Diego, California: Academic Press.

- Grambow, B., Fattahi, M., Montavon, G., Moisan, C., & Giffout, E. (2006). **Sorption of Cs, Ni, Pb, Eu (III), Am (III), Cm, Ac (III), Tc (IV), Th, Zr, and U (IV) on Mx 80 bentonite: An experimental approach to assess Model uncertainty.** *Radiochim. Acta*, 94, 627-636.
- Grim, R. E. (1962). *Applied Clay Mineralogy*. New York: McGraw-Hill Book Company.
- Guldbrand, L., Jönsson, B., Wennerström, H., & Linse P. (1984). **Electrical double layer forces. A Monte Carlo study.** *Journal of Chemical Physics*, 80, 2221.
- Humelnicu, D., Bulgariu, L., & Macoveanu M. (2010). **On the retention of uranyl and thorium ions from radioactive solution on peat moss.** *Journal of Hazardous Materials*, 174, 782.
- Humelnicu, D., Popovici, E., Dvininov, E., & Mita, C. (2009). **Study on the retention of uranyl ions on modified clays with titanium oxide.** *Journal of Radioanalytical and Nuclear chemistry*, 279(1), 131-136.
- Hunter, R. J. (1985). *Foundations of Colloid Science*. New York: Oxford University press.
- Jackson, T. A. (1998). The biogeochemical and ecological significance of interactions between colloidal minerals and trace elements. In A. Parker & J. E. Rae (Eds.), *Environmental Interactions of Clays* (pp. 93-205). Berlin: Springer-Verlag.

- Jönsson, B., Åkesson, T., Jönsson, B., Meehdi, S., Janiak, J. & Wallenberg R. (2009). *Structure and forces in bentonite MX-80*. Svensk kärnbränslehantering AB (SKB).
- Kedziorek, M. A. M., Bourg, A. C. M., & Giffaut, E. (2007). **Hydrogeochemistry of Sn (IV) in the context of radioactive waste disposal: Solubility and adsorption on MX-80 bentonite and Callovo-Oxfordian argillite**. *Physics and Chemistry of the Earth*, 32, 568–572.
- Khan, S. A., ur-Rehman R., & Khan, M. A., (1995a). **Adsorption of Chromium (III), Chromium (VI) And Silver (I) On Bentonite**. *Waste Management*, 15(4), 271-282.
- Kraepiel, A. M. L., Keller, K., & Morel, F. M. M. (1999). **A Model for Metal Adsorption on Montmorillonite**, *Journal of Colloid and Interface Science*, 210, 43–54.
- Lagaly, G. (2006). Colloid clay science. In F. Bergaya, B. G. K. Theng, & G. Lagaly (Eds.), *Handbook of Clay Science* (pp. 141-246). Elsevier, Amsterdam.
- Li, Y. H., Wang, S., Wei, J., Zhang, X., Xu, C., Luan, Z., Wu, D., & Wei, B. (2002). **Lead adsorption on carbon nanotubes**. *Chemical Physics Letters*, 357, 263-266.
- Louvel, F. D., Lapeyre, C., Struillou, R., & Arnould, M. (1993). **Retention mechanisms for toxic cations using artificial confinement barriers of clay-cement mixtures**. *Engineering Geology*, 34, 151-158.

- Lujanienė, G., Motiejnas, S., & Šapolait, J. (2007). **Sorption of Cs, Pu and Am on clay minerals.** *Journal of Radioanalytical and Nuclear Chemistry*, 274(20), 345–346.
- Lumistea, L., Muntera, R., Suttb, J., Kivimäeb, T., & Eensaluc, T. (2012). **Removal of radionuclides from Estonian groundwater using aeration, oxidation, and filtration.** *Proceedings of the Estonian Academy of Sciences*, 61(1), 58–59.
- Malasics, A., Gillespie, D., & Boda, D. (2008). **Simulating prescribed particle densities in the grand canonical ensemble using iterative algorithms.** *The Journal of Chemical Physics*, 128, 124102.
- Manning, B. A., & Goldberg, S. (1996). **MODELING ARSENATE COMPETITIVE ADSORPTION IN KAOLINITE, MONTMORILLONITE AND ILLITE.** *Clays and Clay minerals*, 44(5), 609-623.
- McQuarrie, D. A. (2003). *STATISTICAL MECHANICS*, University Science Books.
- Metropolis, N., Rosenbluth, A. W., Rosenbluth, M. N., Teller, A. H., & Teller, E. (1953). **Equation of State Calculations by Fast Computing Machines.** *Journal of Chemical Physics*, 21, 1087.
- Meunier, A. (2005). *Clays*. New York: Springer.
- Norman, G. E., & Filinov, V. S. (1969). **Investigations of Phase Transitions by a Monte Carlo Method,** *High Temperature*, 7(7), 216-222.

- Oda, C., Ikeda, T., & Shibata, M. (1999). **Experimental studies for sorption behaviour of tin on bentonite and rocks, and diffusion behavior of tin in compacted bentonite.** Japan Nuclear Cycle Development Institute (JNC), JNC TN8400 99 073, Japan.
- Parker, A., & Rae, J. E. (1998). *Environmental Interactions of Clays. Clays and the Environment.* New York: Springer.
- Rouquerol F., Rouquerol J., and Sing K. (1999). *Adsorption by Powders and Porous Solids*, London: Academic Press.
- Schoonheydt, R. A., & Johnston, C. T. (2006). Surface and interface chemistry of clay minerals. In F. Bergaya, B. G. K. Theng, & G. Lagaly, *Handbook of Clay Science* (87-112). Amsterdam: Elsevier.
- Segad, M., Jönsson, B., Åkesson, T., and Cabane, B. (2010). **Ca/Na Montmorillonite: Structure, Forces and Swelling Properties.** *Langmuir*, 26(8), 5782–5790.
- Sommers, M. (2010). *Diseases and Disorders: A Nursing Therapeutics Manual.* F.A. Davis Company.
- Songsheng, L., Hua, X., Mingming, W., Xiaoping, S., & Qiong, L. (2012). **Sorption of Eu(III) onto Gaomiaozhi bentonite by batch technique as a function of pH, ionic strength, and humic acid.** *Journal Radioanal Nucl Chem*, 292, 889-895.
- Stumm, W. (1992). *Chemistry of the Solid-Water Interface.* New York, USA: John Wiley & Sons, Inc.
- Turner, D.R., Pabalan, R.T., & Bertetti, F. P. (1998). **Neptunium (V) sorption on montmorillonite: an experimental study and surface**

- complexation modeling study.** *Clay and Clay Mineral*, 46(3), 256-269.
- Ulrich, H. J., & Degueldre, C. (1993). **The sorption of ^{210}Pb , ^{210}Bi and ^{210}Po on montmorillonite: A study with emphasis on reversibility aspects and on the radioactive decay of adsorbed nuclides.** *Radiochimica Acta*, 62, 81-90.
 - Valleau, J. P., & Torrie, G. M. (1979). **A Monte Carlo study of an electrical double layer.** *Chem. Phys. Lett*, 65, 343–346.
 - Valleau, J. P., & Torrie G. M. (1982). **Electrical double layers. 4. Limitations of the Gouy–Chapman theory.** *Journal of Chemical Physics*, 86, 3251–3257.
 - Verwey, E. J. W., & Overbeek, J. T. G. (1948). *Theory of the Stability of Lyophobic Colloids*. Amsterdam: Elsevier Publishing Company Inc.
 - Volesky, B., & Holant, Z. R. (1995). **Biosorption of Heavy Metals.** *Biofechnol. Prog.*, 11(3), 235.
 - Wang, Y. F., Lin, F., & Pang, W. Q. (2007). **Ammonium exchange in aqueous solution using Chinese natural clinoptilolite and modified zeolite.** *Journal of Hazardous Materials*, 142, 160-164.
 - Weaver, C. E., & Pollard, L. D. (1973). *The Chemistry Of Clay Minerals*. London, New York: Elsevier Scientific Publishing Company Amsterdam.
 - Whitehouse, J. S., Nicholson, D., & Parsonage, N. G. (1983). **A grand ensemble Monte Carlo study of krypton adsorbed on graphite.**

Molecular Physics: An International Journal at the Interface, 49(4), 829-847.

- Windt, L. D., Pellegrini, D., & Lee, J. V. (2004). **Coupled modeling of cement/claystone interactions and radionuclide migration.** *Journal of Contaminant Hydrology*, 68, 165-182.
- [www.skb.se/Templates/ Standard____24109.aspx](http://www.skb.se/Templates/Standard____24109.aspx).
- Yang, K., Yiacoumi, S., & Tsouris, C. (2004). **Electrical Double-Layer Formation.** In *Dekker Encyclopedia of Nanoscience and Nanotechnology*. (pp. 1001).
- Yang, S., Li, J., Lu, Y., Chen, Y., & Wang, X. (2009). **Sorption of Ni (II) on GMZ bentonite: Effects of pH, ionic strength, foreign ions, humic acid and temperature.** *Applied Radiation and Isotopes*, 67, 1600–1608.
- Yu, T, Wu, W. S., & Fan, Q. H. (2012). **Sorption of Am (III) on Na-bentonite: Effect of pH, ionic strength, temperature and humic acid.** *Chinese Chemical Letters*, 23, 1189-1192.
- Zhao, D. L., Feng, S. J., Chen, C. L., Chen, S. H., Xu, D., & Wang, X. K. (2008). **Adsorption of thorium(IV) on MX-80 bentonite: Effect of pH, ionic strength and temperature.** *Applied Clay Science*, 41, 17–23.

جامعة النجاح الوطنية
كلية الدراسات العليا

دراسة الاحتفاظ بالملوثات المتعددة الشحنة في طينة البنتونيت

إعداد

إسراء سليمان فايز مراعبه

إشراف

د. زيد نعيم قمحية

د. خولة نعيم قمحية

قدمت هذه الأطروحة استكمالاً لمتطلبات الحصول على درجة الماجستير في الفيزياء بكلية الدراسات العليا في جامعة النجاح الوطنية في نابلس، فلسطين .

2014

ب

دراسة الاحتفاظ بالملوثات المتعددة الشحنة في طينة البنتونيت

إعداد

إسراء سليمان فايز مراعيه

إشراف

د. زيد قمحية

د. خولة قمحية

المخلص

الأيونات المشعة و ان كانت بتركيز قليل تشكل خطرا على البيئة و خاصة على الإنسان و ذلك بسبب إشعاعاتها القوية و طول فترة نصف العمر. المياه من ضمن الأشياء التي لوثتها المواد المشعة. إحدى الطرق لتتقية المياه هو استخدام الماصات الصلبة لإزالة الملوثات النووية. في كثير من الدول مثل السويد وكندا وفرنسا واسبانيا واليابان يقوم تصميم المستودعات النووية في الطين على أساس الجمع بين الحواجز الطبيعية والحواجز الصناعية للحصول على عزل طويل المدى للملوثات النووية. إحدى الطرق هي وضع النفايات النووية في وعاء من النحاس ثم طمره في طينة البنتونيت تحت الأرض.

في هذا العمل تم التركيز على دراسة امتصاص الملوثات النووية ثلاثية و رباعية التكافؤ بواسطة طينة البنتونيت باستخدام "جراند كانونيكال مونت كارلو محاكاة" (Grand Canonical Monte Carlo simulation). تم تبني النموذج البدائي الذي يمثل فيه الماء بواسطة ثابت العزل الكهربائي. العديد من دراسات المحاكاة (simulation) نفذت لعدد من المتغيرات في النظام من اجل دراسة أثر تغير تركيز المواد المشعة في الماء وكثافة الشحنة السطحية للبنتونيت وشحنة المواد المشعة ودرجة حرارة النظام والقوة الأيونية على قدرة البنتونيت على امتصاص المواد المشعة.

ونتيجة لهذه الدراسة وجد أن متوسط تركيز الأيونات المشعة في الطبقة المزدوجة الكهربائية (electrical double layer) و معامل الامتصاص يتأثران بقوة بالمتغيرات الآتفة الذكر. وبالتحديد وجد أن متوسط تركيز الأيونات المشعة في الطبقة المزدوجة الكهربائية تزداد مع

ت

زيادة كثافة الشحنة السطحية للبتونيت وتركيز الأيونات المشعة في المحلول وشحنتها. بينما متوسط تركيز الأيونات في الطبقة المزدوجة الكهربائية يقل مع زيادة درجة الحرارة و القوة الأيونية. ومن جهة أخرى وجد ان معامل الإمتصاص يقل مع زيادة تركيز الأيونات المشعة في المحلول ومع القوة الأيونية ودرجة الحرارة. غير ان معامل الإمتصاص يظهر سلوكا متزايدا مع زيادة كثافة الشحنة السطحية وشحنة المواد المشعة. وهذه التنبؤات حول سلوك امتصاص المواد المشعة تتوافق بشكل جيد مع العديد من النتائج التجريبية وأحيانا تظهر عدم توافق مع نتائج تجريبية أخرى.